2012-05-03

Cartilage Tissue Engineering Using a Modified Decellularized Porcine Cartilage Scaffold and a Novel Centrifugation Cell Seeding Technique

Christopher M. Scanlon
University of Miami, scanlonc324@gmail.com

UNIVERSITY OF MIAMI

CARTILAGE TISSUE ENGINEERING USING A MODIFIED DECELLULARIZED PORCINE CARTILAGE SCAFFOLD AND A NOVEL CENTRIFUGATION CELL SEEDING TECHNIQUE

By

Christopher M. Scanlon

A THESIS

Submitted to the Faculty
of the University of Miami
in partial fulfillment of the requirements for
the degree of Master of Science

Coral Gables, Florida

May 2012

UNIVERSITY OF MIAMI

A thesis submitted in partial fulfillment of
the requirements for the degree of
Master of Science

CARTILAGE TISSUE ENGINEERING USING A MODIFIED DECELLULARIZED PORCINE CARTILAGE SCAFFOLD AND A NOVEL CENTRIFUGATION CELL SEEDING TECHNIQUE

Christopher M. Scanlon

Approved:

_____	_____
Chun-Yuh Charles Huang, Ph.D.	Terri A. Scandura, Ph.D.
Assistant Professor of Biomedical Engineering	Dean of the Graduate School

_____
Alicia R. Jackson, Ph.D.
Assistant Professor of Biomedical Engineering

_____
Weiyong Gu, Ph.D.
Professor and Chair, Department of Mechanical and Aerospace Engineering

SCANLON, CHRISTOPHER (M.S., Biomedical Engineering)

Cartilage Tissue Engineering Using a Modified Decellularized Porcine Cartilage Scaffold and a Novel Centrifugation Cell Seeding Technique. (May 2012)

Abstract of a thesis at the University of Miami.

Thesis supervised by Professor Chun-Yuh Charles Huang
No. of pages in text. (53)

Cartilage tissue engineering remains a top priority due to the limited intrinsic capacity of articular cartilage for self-repair. In this study, the tissue engineering potential of a decellularized porcine cartilage scaffold, in which the proteoglycans (PG) had also been removed, was evaluated. To increase cell seeding efficiency and improve cell distribution within the scaffold, a novel cell seeding technique using centrifugation and a cell seeding device designed specifically for this technique was developed. The modified porcine cartilage scaffolds were seeded with chondrocytes using the novel cell seeding technique and left in static culture for up to 21 days. A previously described bioreactor system was used to measure the tissue properties of the tissue engineered constructs at 7, 14, and 21 days. The ability of the scaffold to support cell viability and proliferation and extracellular matrix deposition was evaluated at these time points as well by means of live-dead staining, hematoxylin and Safranin-O/eosin staining, and DNA assay measurements. The novel cell seeding technique was also evaluated at 24 hours using these methods. Results indicated that the scaffold was capable of supporting cell viability and proliferation at all time points tested. Furthermore, the scaffold encouraged PG deposition by the seeded chondrocytes, as PG accumulation, as measured by fixed charge density, increased up to 21 days to approximately 30% of that of native tissue. This led to

a corresponding decrease in hydraulic permeability at 21 days. The novel cell seeding technique proved capable of achieving a relatively high cell seeding efficiency (54.1±3.63%) and cell density (14,526±750 cells/mg) as compared to native tissue (6,103±792 cells/mg). However, the seeded cells were heavily concentrated in the superficial regions of the scaffold, and the cell distribution was not as uniform as that of native tissue. Overall, this study indicated that the modified decellularized porcine cartilage scaffold could have applications in the field of cartilage tissue engineering. The novel cell seeding technique using centrifugation and the cell seeding device may provide a promising alternative to static and semi-static cell seeding methods; however, its efficacy in this study was likely somewhat mitigated by the low porosity of the scaffold. Future studies will seek improved cell seeding techniques to further evaluate the potential of this scaffold for use in cartilage tissue engineering.

TABLE OF CONTENTS

LIST OF FIGURES

CHAPTER 1: INTRODUCTION

1.1 Articular Cartilage Biology and Osteoarthritis

Articular cartilage is a connective tissue and subset of hyaline cartilage that lines the articular surface of bones at diarthroidial joints.[1] It is an avascular and aneural tissue, and its main function *in vivo* is to cushion and provide mechanical support for the joints where it is found. Articular cartilage is generally divided into four zones based on morphological and histological assessment: the superficial zone, the transitional zone, the deep zone, and the calcified zone.[2] Although the tissue differs structurally through each of these zones, articular cartilage is primarily composed of type II collagen, proteoglycans, and trace amounts of other non-collagenous proteins, and the primary cell type within the tissue is the chondrocyte.[3] The superficial zone is the outermost and thinnest of all the layers. This region is made up of flattened chondrocytes that are surrounded by densely packed collagen fibrils. The superficial zone possesses the highest water concentration of any of the zones and a relatively low level of proteoglycans. The proteoglycan concentration begins to increase in the transitional zone, and the chondrocytes become rounded, while the collagen fibers exhibit a more random orientation. Moving into the deep zone, the proteoglycan concentration continues to increase to its highest throughout the tissue, and the water content drops dramatically. The chondrocytes in this region are rounded and grouped in columns, and they occupy the lowest volume of all the regions. The collagen fibrils become more densely packed, and they are organized randomly into large bundles. The deep zone is the last region before the tide mark, which separates the superficial cartilage zones from the calcified zone. The tide mark is a curved, uneven band of fibrils that are believed to be the

anchorage point for the collagen fibrils in the deep zone. There are tiny breaks in the fibrils that make up the tide mark, which could be present to allow for the passage of nutrients into the final and innermost layer, the calcified zone. The calcified zone is devoid of proteoglycans and is made up mainly of rounded chondrocytes contained in uncalcified lacunae and large collagen fibrils oriented in a manner that is perpendicular to the articular surface. The calcified zone comes into direct contact with the underlying subchondral bone and represents the deepest layer of articular cartilage. This complex structure is maintained in all diarthroidal joints where articular cartilage is present, but the composition can vary somewhat depending on the location within the joint (i.e. load-bearing region vs. non-load bearing region).[3]

Osteoarthritis (OA) is the term given to a group of mechanical abnormalities that is characterized by the thinning or degradation of articular cartilage and the underlying bone.[4] Typical symptoms of the disease include pain or stiffness in the joints, especially following periods of heavy activity or no activity, a grating sensation that is felt during the movement of the joints, and joint effusion. However, the disease can be extremely debilitating and can worsen to the point where it affects one's ability to lead a normal lifestyle or remain gainfully employed.[5] In fact, OA affects almost 27 million Americans and costs the U.S. economy over $128 billion every year in lost wages and productivity.[6,7] Although there are several known risk factors related to osteoarthritis, such as genetics, obesity, and fractures or other joint injuries, in many cases, the direct cause of the disease is unknown.[4] Furthermore, at present, there is no cure for osteoarthritis, and current treatments, which include analgesics, exercise, lifestyle changes, and physical therapy, do little to stop the progressive worsening of the disease.[8]

The final treatment option when lifestyle modifications have failed to alleviate the symptoms of OA is microfracture surgery or total knee replacement surgery.[4] However, these treatments are avoided if possible, as microfracture surgery requires causing further damage to the injury site, and the artificial joint that is implanted during total knee replacement surgery often fails after 10 to 15 years.[9,10] The largest obstacle to the treatment of osteoarthritis is the inability of the damaged articular cartilage to repair itself.[10] Unlike other tissues that, for the most part, have some capacity for self-repair, articular cartilage is often unable to regenerate after it has become diseased or damaged.[10,11] This is due to a variety of reasons which are discussed below.

1.2 Obstacles for Self-Repair of Articular Cartilage

While the density of chondrocytes within articular cartilage varies from zone to zone, in general, chondrocytes occupy only about 5% of the volume of articular cartilage.[12] This heavily contributes to the inability of cartilage to be regenerated once it has been damaged or destroyed.[10] Since the chondrocytes that populate articular cartilage are the only means by which new tissue can be created in the event of osteoarthritis, the scarcity of these cells distributed throughout the tissue severely limits the production of new extracellular matrix (ECM) components to replace those that have been lost.[13] The lack of vascularization within articular cartilage further contributes to its limited capacity for self-repair.[10] Whereas in other tissues blood vessels allow for the transport of adult stem cells to the affected area, if the underlying subchondral bone is not damaged, there are limited means for progenitor cells that could replace those cells lost due to tissue damage to migrate to the injury site.[9,14] Furthermore, chondrocytes' mechanism for producing new ECM components is an anabolic process that requires the consumption of

nutrients (i.e., glucose, oxygen).[15] Due to the avascular nature of the tissue, nutrient transport within articular cartilage occurs primarily through diffusion from the synovial fluid.[16] Since articular cartilage is a relatively thick and dense tissue, this severely limits the rate of nutrient transport within the tissue. This is thought to not only contribute to the development of OA initially, as cell viability and ECM biosynthesis decrease with the onset and progression of OA, which is thought to be a factor of the inadequate nutrient supply, but also limit the ability of the cells to remodel the tissue in the event of tissue damage.[10,17,18] It has also been shown that, while healthy chondrocytes obtained from osteoarthritic joints are capable of upregulating the production of ECM macromolecules, these cells also demonstrate a similar increase in catabolic signaling pathways, which prevents the accumulation of ECM components in the extracellular space.[19] This suggests the possible presence of a more widespread metabolic disorder that could be the cause of osteoarthritis in some older patients and indicates that the chondrocytes in osetoarthritic cartilage could be incapable of synthesizing ECM molecules in sufficient quantities to repair damaged cartilage. Since cartilage has little to no ability to regenerate itself once it has become diseased or damaged, tissue engineering has been sought as a means to replace the affected tissue.[20]

1.3 Tissue Engineering for Repair of Articular Cartilage

Tissue engineering provides the potential to develop many different types of replacement tissues for those that are damaged or no longer functional.[20-22] Cartilage tissue engineering could have widespread applications, as the previously discussed limited capacity of cartilage for self-repair necessitates the use of a tissue replacement to alleviate the symptoms of OA.[20] Recognizing the limitations of past treatments, scientists

and clinicians recently pioneered the use of autologous chondrocyte implantation (ACI) for the treatment of osteoarthritis and other cartilage defects.[23] ACI involves removing a small piece of articular cartilage from a non-load bearing site, usually the femoral chondyle, in the joint where the defect is present.[23] The biopsied tissue is then enzymatically digested to allow for isolation of the patient's own chondrocytes, and after expansion, the chondrocytes are implanted into the defect site and covered with a piece of periosteum harvested from the patient's tibia.[23] While this technique has been used extensively with positive, although varying, results, ACI has many drawbacks including donor site morbidity, the need for two separate surgeries, and difficulty in retaining the implanted chondrocytes at the defect site.[24] Treatments like ACI, microfracture surgery, and total knee replacement surgery provide a more comprehensive solution to OA, in that these treatments seek to repair the cause of OA rather than simply treating the symptoms.[4,10,23] However, tissue engineering provides this possibility, as well as the possibility of a non-autogenic source of replacement tissue, which would eliminate the need for additional surgeries and any donor site morbidity.[25]

Current cartilage tissue engineering approaches typically involve developing a man-made scaffold that mimics the *in vivo* environment of chondrocytes and seeding the developed scaffold with autologous or allogeneic stem cells or chondrocytes.[11,25] These scaffolds vary in their composition but generally consist of natural or synthetic materials that are native to the cartilage ECM or similar to components within the ECM.[26] The most commonly used materials for these scaffolds are type I and type II collagen, alginate, agarose, chitosan, chondroitin sulfate, fibrin and hyaluronic acid (or hyaluronan).[27-29] Furthermore, there are a multitude of polymers that are currently being

investigated for use in designing scaffolds, such as polycaprolactone (PCL), poly(ethylene glycol), and poly(lactic-co-glycolic acid)(PLGA).[30-32] All of these materials can be extensively modified to design scaffolds with varying structures and properties.[27-32] The majority of approaches involve either forming a cross-linked network of one or more of these materials that results in the formation of a hydrogel or developing a porous composite scaffold through a number of methods such as chemical cross-linking, freeze-drying, particulate leaching, rapid prototyping, or electrospinning.[28,33-38] While all of these methods have been shown to have the ability to create scaffolds that support cell viability and matrix production, no currently developed scaffold has been identified as the ideal choice for cartilage tissue engineering.[11] This is due to a number of reasons, as each scaffold has its own limitations. Hydrogels are relatively easy to construct and could present a less-invasive means by which to deliver new cells to the defect site arthroscopically; however, constructs that make use of hydrogels lack the necessary mechanical strength to provide support to the cells and the surrounding tissue.[39] Furthermore, many hydrogel constructs suffer from the same cellular retention problems that are experienced with ACI.[40]

Many porous composite scaffolds have been developed with similar properties and mechanical strength to that of native tissue.[26] However, the complex makeup of the articular cartilage ECM is difficult to mimic using man-made scaffolds, which often leads to poor integration into the defect site and can ultimately lead to rejection of the tissue engineered construct.[26,41] Due to the intricate nature of cartilage tissue, some tissue engineering approaches have sought to use decellularized cartilage as a scaffold.[42-44] This technique has not been widely used, however, as the compact nature of the cartilage ECM

makes recellularizing the scaffolds extremely difficult. All studies that have been reported so far utilizing a decellularized cartilage scaffold have shown limited cellular integration into the scaffold, as the majority of the seeded cells remain in the superficial layers of the scaffold. Yang et al. circumvented this problem by physically shattering the cartilage ECM and cross-linking the resulting fragments using carbodiimide to create scaffolds.[45] Through this method, they were able to create scaffolds with increased porosity, but their method resulted in the loss of the physical structure of the ECM leaving it prone to the same shortcomings as other porous composite scaffolds. Previous studies used static or semi-static techniques to seed the decellularized cartilage scaffolds.[42-44] This could be the primary reason that limited cellular integration was seen, as these techniques have been shown to be inefficient at achieving a uniform cell distribution throughout a scaffold.[46-49]

1.4 Rationale of Current Study

In accordance with the limitations of current cartilage tissue engineering approaches, this study sought to develop a novel scaffold and cell seeding technique that would allow for the development of tissue engineered constructs that more closely mimic native articular cartilage. The extremely dense nature of the cartilage ECM accounts for the majority of the difficulties that arise during cell seeding of decellularized cartilage scaffolds, as this limits the ability of the cells to be seeded into the deeper layers of the scaffold.[45] To help alleviate this problem, one component of the cartilage ECM could be removed in an attempt to increase the porosity. Toolan et al. developed a protocol for decellularizing bovine osteochondral plugs and removing the proteoglycans without disturbing the collagen matrix.[43] The authors then attempted to recellularize the graft

through lyophilization and subsequent rehydration in a solution containing chondrocytes. Using this technique, the authors observed improved healing of full-thickness articular cartilage defects, when compared to defects that were not treated, with minimal inflammatory response even in a xenograft model. However, integration of the cells into the decellularized tissue was limited, as the seeding occurred in static culture, and the cells were not able to migrate into the deeper layers of the grafts. The complexity of the graft made it difficult to develop alternative cell seeding strategies to improve the cell distribution.

While this approach may not be suitable for osteochondral tissue engineering, a similar protocol can be used to create a scaffold for cartilage tissue engineering that does not include any underlying bone. This scaffold would still exhibit many advantages for use in cartilage tissue engineering. Removing the PG portion of the cartilage ECM increases the porosity of the scaffold, making it more feasible to achieve a uniform cell distribution throughout a tissue engineered construct.[43] Furthermore, while the PG composition of cartilage is important in providing compressive resistance[50], the intricate collagen network is primarily responsible for the mechanical strength and integrity of the tissue.[51] Achieving a mechanical strength that is similar to that of native articular cartilage is vital to the success of cartilage tissue engineered constructs, as one of the primary functions of the tissue *in vivo* is providing mechanical support.[11] Many cartilage tissue engineered constructs fail due to a lack of mechanical strength which prevents them from functioning properly when implanted. It has also been recently shown that proper crosslinking of collagen is as important as collagen content for the tissue to maintain its functional properties.[51,52] This natural crosslinking may be difficult to mimic

using manmade scaffolds, which suggests that it may be more important to maintain the structure of the collagen network than to maintain the PG matrix to achieve a suitable tissue engineered construct that possesses the mechanical strength of native cartilage.[51] Although PG do not play as significant of a role as the collagen network in the mechanical strength of cartilage, it is vital that tissue engineered constructs have a well-defined PG matrix similar to that of native tissue for the construct to function properly *in vivo*.[29] However, studies suggest that removing the PG component of the cartilage ECM has advantages over interfering with the collagen matrix.[53-58] It has been shown extensively that chondrocytes produce more PG than type II collagen *in vitro*[53,57] and *in vivo*[55], indicating that seeded chondrocytes could be able to quickly redeposit the PG matrix that was removed. Furthermore, type II collagen used as a medium supplement and as a three-dimensional scaffold helped restore the chondrocyte phenotype in chondroctyes up to P7 and increased glycosaminoglycan production in these cells, while other ECM molecules that make up the PG component of cartilage such as chondroitin sulfate and hyaluronic acid did not.[56] Finally, for tissue engineering purposes, it is desirable for a scaffold to support the differentiation and maintenance of a differentiated phenotype of stem cells, so that stem cells can ultimately be used as the cellular component of the tissue engineered construct.[11,20] Maintenance of the chondrocyte phenotype is especially important for cartilage tissue engineering, as chondrocytes are particularly quick to lose their phenotype during expansion.[59] Scaffolds and hydrogels composed of type II collagen have been shown to induce and support the differentiation of mesenchymal stem cells both *in vitro*[54] and *in vivo*[58] and both with[54] and without[58] treatment with growth factors, outperforming alginate and type I collagen hydrogels[54] and

collagen-alginate composite scaffolds[58]. Many studies have also demonstrated that culturing stem cells in an environment similar to that of *in vivo* cartilage can promote and support chondrogenesis.[60] Since the complex structure of the mostly type II collagen matrix would still be intact, this scaffold could be expected to support chondrogenic differentiation and maintenance of the chondrocyte phenotype. For all of these aforementioned reasons, it is reasonable to suggest that a decellularized cartilage scaffold would retain many desirable qualities as a scaffold for cartilage tissue engineering even when the PG component has been removed.

Even with the removal of the PG component, the cartilage ECM remains extremely dense.[43] Difficulties in seeding cells into scaffolds composed of decellularized cartilage ECM have led many to abandon their use entirely.[42,43,61] While this appears to be a prevailing problem for scaffolds of this type, few studies have used dynamic cell seeding techniques to improve cell integration into the scaffold.[61] As noted above, it has been shown extensively that static and semi-static cell seeding techniques are inefficient and are particularly poor at seeding cells in a uniform manner throughout a scaffold.[46-49,62] Achieving a uniform cell distribution throughout a scaffold and a cell density similar to that of native tissue is imperative to the function of tissue engineered constructs *in vivo*.[11,20] Also, seeding the cells at a high initial density can have a strong effect on the production of ECM by the seeded cells and may even be more important than the stage of cell differentiation, as two recent studies have shown that increasing the cell seeding density can lead to drastic increases in the production of both type II collagen and glycosaminoglycans.[63,64] Cell seeding using centrifugation has been shown to be an inexpensive and simple method for increasing cell seeding efficiency and improving

cellular integration into the deeper layers of scaffolds, although its use for cartilage tissue engineering has been limited.[46,65-68] There are many variations of this technique[66], but one of the more common ones involves suspending the scaffold with a cell solution added on top and then centrifuging the scaffold and cell solution in a tube.[46] The rationale behind this technique is that the centrifugal force will force the cells into the deeper layers of the scaffold rather than allowing them to just bind to the surface of the scaffold which often happens in static culture.[46,66] Cell seeding using centrifugation could have applications in cartilage tissue engineering, especially when using a scaffold with low porosity, such as the scaffold discussed above. The centrifugal force acting on the cells during centrifugation should increase the cell seeding efficiency as well as the cell density in the deeper levels of the scaffold. Even if the scaffold is too dense and the majority of the cells are seeded in the superficial layers, this technique could still have advantages over static cell seeding techniques. The seeded cells could begin to migrate into the deeper layers of the scaffold in culture due to the high density of cells in the superficial layer, and by quickly seeding the cells in the superficial layers using this technique, this migration could be accelerated.

In this study, a scaffold composed of decellularized porcine cartilage was modified by removing the PG component of the ECM. The tissue engineering potential of this scaffold was then tested by recellularizing the scaffold with chondrocytes and evaluating the properties of the constructs after long-term static culture. To address the cell seeding difficulties that were encountered when using similar scaffolds[42-44], a novel cell seeding technique using centrifugation was developed. A cell seeding device that was designed specifically to suspend the modified scaffold during centrifugation was created

for use with this technique. The cell seeding efficiency and cell distribution within the scaffold that was achieved using this novel cell seeding technique was also assessed.

CHAPTER 2: MATERIALS AND METHODS

2.1 Cell Isolation and Expansion

Porcine articular chondrocytes were isolated from the proximal and distal head of the porcine humerus as previously described.[69] Briefly, the humeri of 4-to 6-month-old pigs obtained from a local slaughterhouse were removed within approximately 2 hours of sacrifice. Cartilage from the articulating surfaces of the humeri was removed under a sterile hood and was finely chopped before being incubated in an enzyme solution containing Dulbecco's modified Eagle's medium (DMEM, Invitrogen Corp., Carlsbad, CA) supplemented with 10% fetal bovine serum (FBS; Invitrogen Cor.), 1% antibiotic-antimycotic (Atlanta Biologicals, Inc., Lawrenceville, GA), collagenase type II (1.5 mg/ml; Worthington Biochemical Corp., Lakewood, NJ), and protease (0.6 mg/ml; Sigma Aldrich, St. Louis, MO). The tissue was cultured in the enzyme solution at 37°C and 5% CO_2 for up to 48 hours at which point any remaining undigested tissue was removed using a 70 μm filter (BD Biosciences, San Jose, CA). The chondrocytes were then cultured and expanded at 37°C and 5% CO_2 in DMEM supplemented with 10% FBS and 1% antibiotic-antimycotic. Cells were used up to P3.

2.2 Scaffold Preparation

Scaffolds (d=8mm, h=1mm) were prepared from the articular cartilage on the proximal and distal head of the porcine humerus. Porcine humeri were obtained as described above. However, select humeri were frozen at -20°C to use for scaffold preparation. After the tissue was frozen for at least 48 hours, the porcine humeri were thawed, and 45 articular cartilage samples were obtained using a previously described method.[70] Briefly, articular cartilage samples (d=8 mm, h=1 mm) were prepared using an

8 mm corneal trephine (Biomedical Research Instruments, Inc., Silver Spring, MD) and a sledge microtome (Model SM2400, Leica Instruments, Nussloch, Germany) with freezing stage (Model BFS-30, Physitemp Instruments, Inc., Clifton, NJ). To prepare the cartilage samples for use as scaffolds, the samples were decellularized, and the proteoglycans were removed using a protocol adapted from Toolan et al.[43] The samples were first placed in 1 ml of a digestion solution containing hyaluronidase (3 mg/ml; Worthington Biochemical Corp., Lakewood, NJ) and trypsin (2.5 mg/ml; Sigma Aldrich, St. Louis, MO). The samples were then sonicated in the digestion solution for 18 hours at 37°C and 5% CO_2. After 18 hours, the scaffolds were removed and washed with DD H_2O three times and then placed in a 50%/50% chloroform-methanol solution for 72 hours at room temperature to remove the remaining cellular debris and sterilize the scaffolds. Finally, the scaffolds were washed three times with DD H_2O and left in phosphate buffered saline (PBS; Sigma Aldrich, St. Louis, MO) under sterile conditions until they were seeded.

2.3 Cell Seeding

All scaffolds were seeded using centrifugation and a novel cell seeding device developed to facilitate seeding via centrifugation. The cell seeding device (Fig. 1) is composed of polycarbonate and consists of two cylindrical pieces that are approximately 26.36 mm in height together and 9.50 mm in diameter. The two pieces differ in height with the smaller piece being approximately 11.66 mm in height and the large piece being approximately 14.70 mm in height. The diameters of both pieces are identical. The center of the two cylindrical pieces has been removed to form a hollow cylinder that runs from the top to the bottom of the two pieces. The diameter of the inner cylinder that has been

removed is approximately 6.70 mm. The smaller piece is uniformly cut from top to bottom. However, the larger piece differs at one end to allow for the scaffold to be secured within the device. At this end, the diameter of the inner cylinder that has been removed is 8 mm. The height of this portion of the cylinder that has been removed is 1 mm. This allows the scaffold to be suspended between the two cylindrical pieces during cell seeding. The cell seeding device is designed to fit securely in a Cryo.s™ 2 ml freezing tube (Greiner Bio-one, Frickenhausen, Germany).

The procedure that was used to seed the scaffolds is as follows. The isolated chondrocytes were trypsinized and suspended at a concentration of $3.0x10^6$ cells/milliliter. The scaffolds were then loaded into the cell seeding device, and the device was loaded into the Cryo.s™ 2 ml freezing tubes so that the smaller piece was at the bottom of the tube and the larger piece was placed on top with the end where the scaffold was loaded closest to the bottom of the tube. This allowed the scaffold to be suspended between the smaller piece and the larger piece in the middle of the freezing tube. Then, a volume of 250 μl of the cell solution was added on top of the suspended scaffold inside the larger piece of the cell seeding device. Once the freezing tube was closed after the cell solution was added, the seeding device was designed to be secure enough within the tube to not allow the cell solution to escape from the top of the larger piece. The cell seeding devices inside the freezing tubes were then centrifuged at 1000 rpm and 4°C for 4 minutes. After the 4 minutes had passed, the cell seeding devices were checked to make sure that the scaffold had not become dislodged during centrifugation. In the event that the scaffold became dislodged, the scaffold was positioned back in the cell seeding device, and the remaining cell solution was added on top of the scaffold.

Then, the freezing tubes were centrifuged again at 1250 rpm and 4°C for 4 minutes. Again, the cell seeding devices were inspected to determine if the scaffold had become dislodged, and the freezing tubes were then centrifuged again at 1500 rpm and 4°C for 4 minutes. After this centrifugation cycle was complete, the scaffolds were inverted and repositioned in the cell seeding devices in the same manner with the opposite side facing the top of the freezing tube. Another 250 µl of the cell solution was added on top of the scaffold, and the freezing tubes were then put through the same centrifugation cycle. The concentration of the cell solution was determined before each centrifugation cycle, and the concentration of the cell solution remaining in the freezing tubes following the centrifugation cycle was checked as well. Following this, the scaffolds were placed in six-well plates (Greiner Bio-one, Frickenhausen, Germany) containing DMEM supplemented with 10% FBS and 1% antibiotic-antimycotic. The scaffolds were left in static culture at 37°C and 5% CO_2 until they were removed for analysis, and the cell concentration in the culture medium was checked periodically to determine the ability of the scaffold to retain the seeded cells.

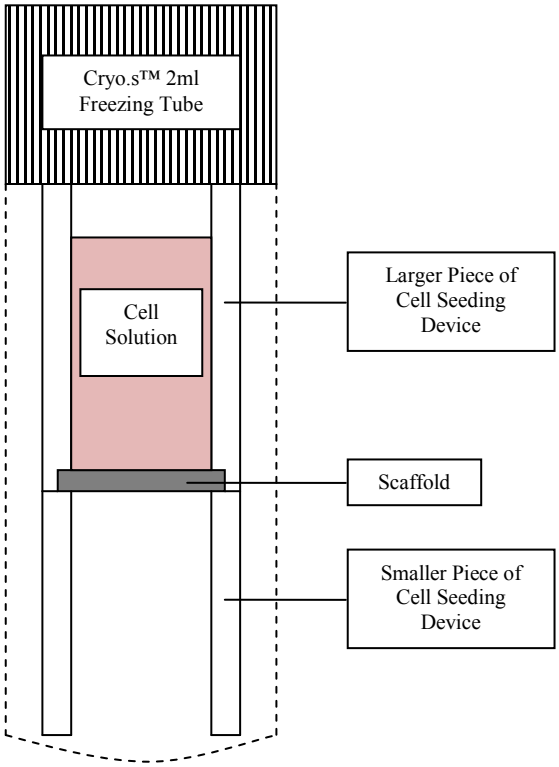

Figure 1. The novel cell seeding device. The bottom of the larger piece has a "shelf" that is 8mm in diameter and 1 mm in height. The scaffold was placed here during cell seeding, and the smaller piece was placed below the larger piece in the tube to provide support to the scaffold during seeding. The device was designed to fit into the Cryo.s™ 2ml freezing tube, so that the medium could not escape from the top of the larger piece when the cap of the freezing tube was secure.

2.4 Bioreactor Group

2.4.1 Bioreactor Measurements

Tissue-engineered constructs (n=6 for each time point) were removed at 7, 14, and 21 days after cell seeding and placed into the Bioreactor group. These constructs were frozen at -80°C before being tested using a previously described bioreactor and protocol.[70] Briefly, the samples were loaded into the bioreactor in which they were bathed in PBS, and a 10% level of compressive strain was applied. After the system was allowed to equilibrate, a 10μA current was applied across the samples, and the conductivities of the samples were measured by determining the resistance across the

tissue using Ag/AgCl electrodes. The water volume fraction or porosity (Φ^w) of the constructs was calculated using this measurement according to the following equation[70]:

$$\Phi^w = \frac{\chi RT}{F_c^2(c^+D^+ + c^-D^-)} \quad (1)$$

where χ is the conductivity of the construct, R is the universal gas constant, T is the temperature at which the measurements were performed (298 K), F_c is Faraday's constant, c^+ is the concentration of Na^+ within the tissue, D^+ is the diffusivity of Na^+ within the tissue, c^- is the concentration of Cl^- within the tissue, and D^- is the diffusivity of Cl^- within the tissue. The ion concentration and diffusivity in the tissue were calculated using the following equations[70,71]:

$$c^+ = \frac{c^F + \sqrt{(c^F)^2 + 4(c^*)^2}}{2} \quad (2)$$

$$c^- = \frac{-c^F + \sqrt{(c^F)^2 + 4(c^*)^2}}{2} \quad (3)$$

where c^F is the fixed charge density of the sample, and c^* is the concentration of NaCl in the PBS solution.

$$D^{\pm} = D_0^{\pm}\, exp\left[-1.25\left(\frac{r_{\pm}}{\sqrt{\kappa}}\right)^{0.681}\right] \quad (4)$$

where D_0 is the ion diffusivity in free solution, r_+ and r_- are the radii of Na^+ and Cl^-, respectively, κ is the Darcy permeability (calculated by multiplying the hydraulic permeability, k, by the viscosity of PBS), and the constants -1.25 and 0.681 were determined experimentally.[71]

Next, a fluid pressure difference of 7.5 psi was applied across the constructs, and the fluid flow and streaming potential was measured using a digital flow meter and the Ag/AgCl electrodes, respectively. These measurements were used to calculate the

hydraulic permeability (k) and fixed charge density (c^F) of the tissue engineered constructs using the following equations[70]:

$$k = \frac{Qh}{\Delta pA} \quad (5)$$

where Q is the measured flow rate across the construct, h is the height of the construct, Δp is the applied pressure across the construct, and A is the area of the circular end of the cylindrical constructs;

$$c^F = \frac{-\Delta\psi\chi}{F_c\Delta pk} \quad (6)$$

where $\Delta\psi$ is the measured streaming potential and k is the hydraulic permeability as calculated by Equation 6.

Additionally, one undigested sample and one sample digested using the digestion solution consisting of hyaluronidase and trypsin was tested using the bioreactor to serve as a positive and negative control, respectively.

2.4.2 Water Content and Fixed Charge Density Analysis

After the constructs had undergone testing with the bioreactor, the samples were immediately weighed and frozen at -80°C. They were then lyophilized and reweighed before being digested using a papain solution consisting of sodium phosphate (100 mM; Sigma Aldrich, St. Louis, MO), ethylenediaminetetraacetic acid (EDTA; 10 mM; Sigma Aldrich, St. Louis, MO), cysteine HCl (10 mM; Sigma Aldrich, St. Louis, MO), and papain (250 μg/ml; Sigma Aldrich, St. Louis, MO) for 24 hours at 65°C. After the constructs were fully digested, dimethylmethylene blue (DMMB) assay was performed to determine the fixed charge density of the constructs. The DMMB assay is capable of determining the equivalent chondroitin sulfate (CS) content of a given sample.[72] One hundred microliters of the digested construct solution was reacted with 1.9 ml of DMMB

solution in a disposable cuvette. The sulfated GAG content was then measured spectrophotometrically at 525 nm. A standard curve for this test was created using bovine chondroitin sulfate A (Sigma Aldrich, St. Louis, MO). The measured value was used to calculate the FCD of the constructs based on the quantity of charge per fluid volume of the constructs, assuming a molecular weight of 502.5 g/mol of CS and two moles of charge per mole of CS.[73,74] Three additional undigested samples underwent these procedures (but not the Bioreactor Measurement procedures) to serve as a reference point for the FCD and water content of native tissue. With an assumption that the density of water (ρ_w) is approximately equal to the density of the sample (ρ_t), the water volume fraction (Φ^w) of the tissue can be used to approximate the water content of the tissue which can be determined after lyophilization.[70]:

$$\Phi^w = \frac{v_w}{v_t} = \frac{w_w/\rho_w}{w_t/\rho_t} = \frac{w_w}{w_t}\frac{\rho_t}{\rho_w} \cong \frac{w_w}{w_t} \quad (7)$$

where v_w is the volume of the water in the sample, v_t is the total volume of the sample, w_w is the weight of the water present in the sample and was determined by subtracting the weight of the sample after lyophilization from the weight of the sample before lyophilization, w_t is the weight of the sample before lyophilization, ρ_w is the density of water, and ρ_t is the density of the sample.

2.5 Histology Group

2.5.1 Live-dead Staining

Additional constructs were removed at 24 hours (n=3), 7 (n=4), 14 (n=4), and 21 (n=6) days after cell seeding and placed into the Histology group. Two additional scaffolds that had undergone digestion using the digestion solution containing hyaluronidase and trypsin also underwent all of the following procedures. The weights of

the constructs were recorded before any of the histology procedures were performed. Next, the constructs were cut in half using a Tissue-Tek® Accu-Edge trimming knife with short handle (Sakura Finetek USA, Inc., Torrance, CA). Two Accu-Edge 130 mm blades (Sakura Finetek USA, Inc., Torrance, CA) were loaded into the holder. This technique allowed the samples to be cut in half, yielding two half discs and one transverse, full-length section that is approximately 60 microns wide. Live-dead staining was performed on this 60-micron wide, full-length transverse section using a LIVE/DEAD® Viability/Cytotoxicity Kit containing calcein AM and ethidium homodimer (Invitrogen Corp., Carlsbad, CA) according to the manufacturer's protocol. The sections were imaged on an Olympus® IX70 Fluorescence Microscope (Olympus America Inc., Center Valley, PA) with a FITC and Texas Red excitation filter (Olympus America Inc., Center Valley, PA). Microscopic images were captured using a Retiga 200R Fast 1394 Color Camera (Quantitative Imaging Inc., Surrey, British Columbia) and QCapture Pro 6.0 imaging software (Quantitative Imaging Inc., Surrey, British Columbia). Three samples of native cartilage were also harvested from the articular cartilage on the proximal and distal head of the porcine humerus within two hours of sacrifice, and a thin, transverse section was removed from the center of the tissue, yielding two half discs along with the transverse section. These thin sections underwent the same protocol for live-dead staining as the sections taken from the constructs.

2.5.2 Hematoxylin and Safranin-O/Eosin Staining

One of the two remaining halves of the constructs was fixed in formalin for 72 hours for histology. After fixation, the samples were dehydrated in graded steps of ethanol (70%, 80%, 95%, and 100%), washed in xylene, and cast in paraffin. The

samples were then sectioned at 5 μm using a Shandon Finesse 325 Microtome (Thermo Fisher Scientific, Middletown, VA), mounted on VWR Superfrost® Plus Micro Slides (VWR International, West Chester, PA) and stained with either hematoxylin and eosin or hematoxylin and Safranin-O. The sections were visualized on an Olympus BX50 Differential Interference Contrast Microscope (Olympus America Inc., Center Valley, PA) at 10x and 20x magnification. One half of the three native tissue samples from above was immediately fixed in paraffin and was also stained with hematoxylin and Safranin-O following the same protocol.

2.5.3 DNA Quantification

The other remaining halves of the constructs were weighed and placed in a papain solution consisting of sodium phosphate (100 mM), EDTA (10 mM), cysteine HCl (10 mM), and papain (250 μg/ml) for 24 hours at 65°C. After digestion, the DNA content of the samples was measured using a Quant-iT™ dsDNA BR Assay Kit (Invitrogen Corp., Carlsbad, CA) and a Qubit® Fluorometer (Invitrogen Corp., Carlsbad, CA). A standard curve (10 points from $0.2x10^6$ to $2.0x10^6$ cells) for this measurement was created using lysis buffer and P2 chondrocytes. Two samples were used for each point on the standard curve, and two readings were taken for each sample. The other half of the three native tissue samples was immediately placed in the same papain solution as described above, and DNA measurements were performed following the same protocol.

CHAPTER 3: RESULTS

3.1 Preliminary Measurements

3.1.1 Initial Scaffold Characterization

One scaffold that had been digested using hyaluronidase and trypsin was tested using the bioreactor to serve as a negative control. The absence of proteoglycans in the digested scaffold was predicted by the lack of a measured streaming potential during the bioreactor testing. This was confirmed using DMMB, as the PG content was below the measurable threshold of the test. The hydraulic permeability and the water content of the digested scaffold were also measured using the bioreactor and were found to be 1.45×10^{-14} m^4/NS and 0.929, respectively. The DNA content of two additional digested scaffolds was determined to ensure that complete decellularization of the scaffolds was achieved. The DNA content of both of the digested scaffolds was undetectable using the Quant-iT™ dsDNA BR Assay Kit (Invitrogen Corp., Carlsbad, CA). The absence of proteoglycans and cells within the digested scaffolds was further confirmed through histological staining with hematoxylin and Safranin-O. Sections of digested scaffolds showed a much less dense matrix with the absence of hematoxylin staining for cell nuclei when compared to scaffolds that had not undergone digestion (Fig. 1). Furthermore, the characteristic intense red staining of the PG matrix by the Safranin-O was not visible in scaffolds that had undergone digestion (Fig. 1).

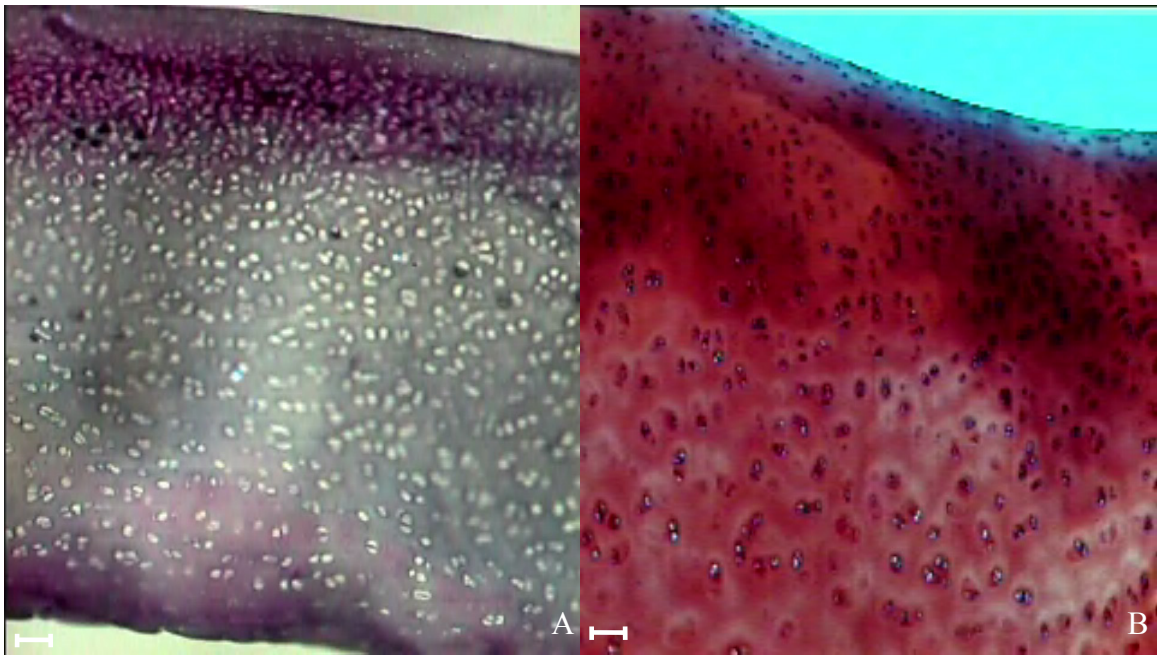

Figure 2: Representative images of the histological appearance of a digested scaffold (A) and an undigested scaffold (B). Both sections stained with hematoxylin and Safranin-O. Images are shown at 10x magnification. Scale bars =125 µm.

3.1.2 Characterization of Native Tissue

An additional sample that had not been digested was tested using the bioreactor to determine the tissue properties of native tissue. The FCD of the undigested sample was measured to be 141.41 moles/m^3 using the bioreactor system and 142.47 moles/m^3 using the DMMB assay. The FCD and water content of three additional undigested samples was determined to serve as a reference point. Including all cartilage samples that were tested (n=4), the PG content of native tissue, as expressed in terms of FCD, was determined to be 141.17±31.26 mole/m^3, and the water content was determined to be 0.735±0.047. Three additional samples of live tissue were obtained, and the DNA content of these samples was measured and normalized by weight. Based on these measurements, the cell density of native tissue was determined to be 6,103±792 cells/mg. The measurements that were taken for native tissue were used for comparison to that of the measurements taken of the tissue engineered constructs.

3.2 Bioreactor Measurements

Tissue engineered constructs (n=6 at each time point) were removed from culture at 7, 14, and 21 days, and the tissue properties were measured using the bioreactor system. Measurements obtained using the bioreactor showed a consistent increase in FCD within the constructs from baseline up to the 21 day endpoint. This was verified through DMMB quantification, which indicated a similar increase in FCD over the 21 day period (Fig. 2). However, the total accumulation of PG in the scaffolds at 21 days was only about 30% of the measured FCD of native tissue (141.17±31.26 mole/m^3).

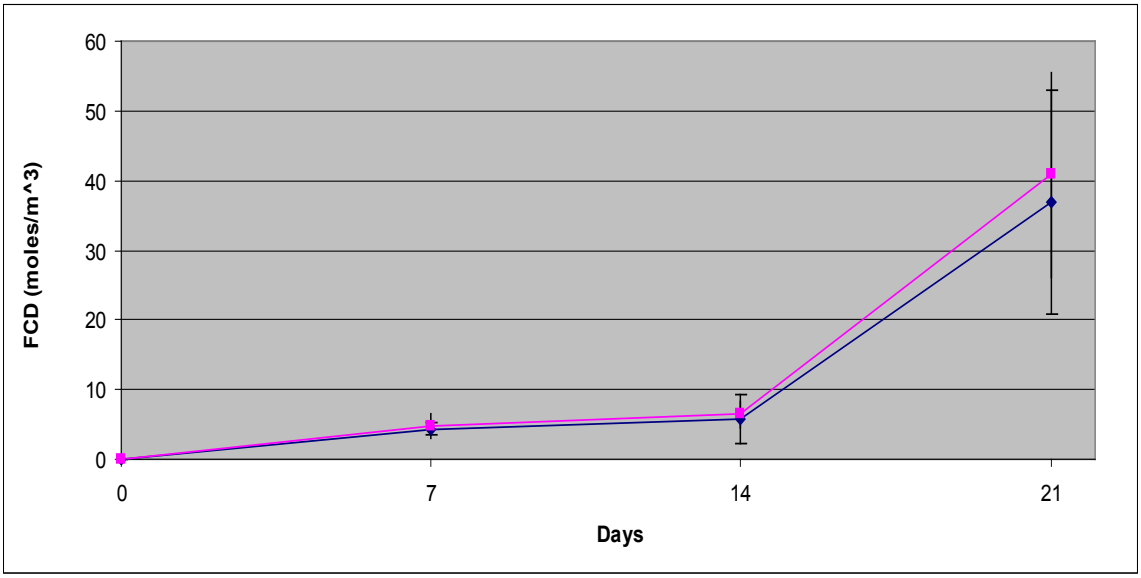

Figure 3: Comparison of the FCD measured with the bioreactor (■) to that measured using DMMB quantification (♦). Data are shown at 7 (n=6), 14 (n=6), and 21 (n=6) days. Error bars show ±standard deviation.

This increase in PG production was accompanied by a decrease in the hydraulic permeability of the constructs, as measured by the bioreactor system (Fig. 3). While there seemed to be little change in the hydraulic permeability of the constructs from baseline at 7 and 14 days, there was a large decrease in the hydraulic permeability to $5.01x10^{-15}$±$1.23x10^{-15}$ m^4/Ns at 21 days that corresponded with the significant increase in PG

content in these samples. This value was approximately an order of magnitude higher than that of native tissue ($0.16x10^{-15}m^4/Ns$).

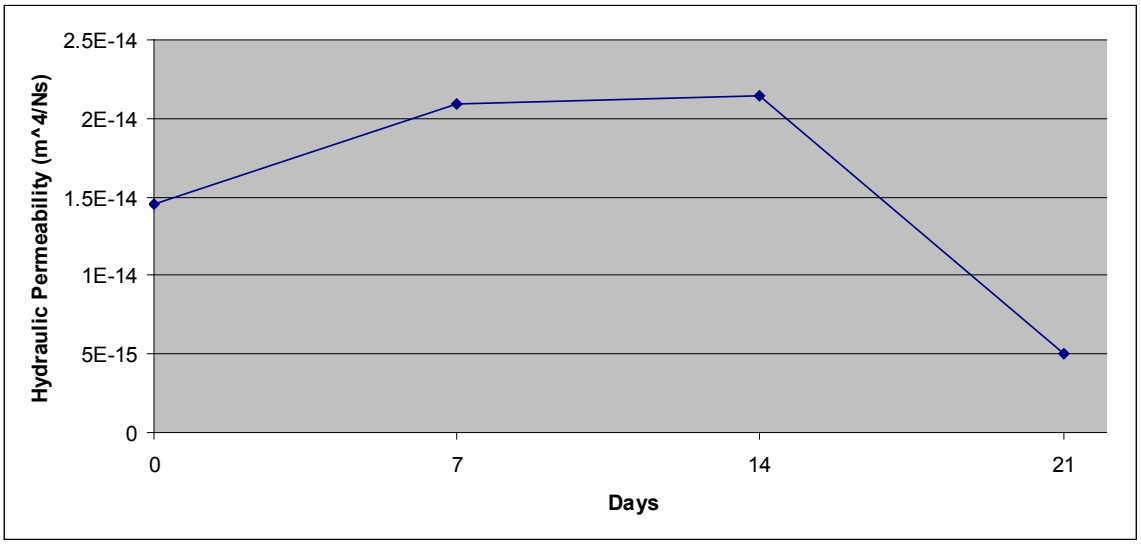

Figure 4. Hydraulic permeability of scaffold at baseline and tissue engineered constructs. Data are shown for the scaffold at baseline (n=1) and at 7 (n=6), 14 (n=6), and 21 days (n=6). Error bars show ±standard deviation.

The water content of the constructs was also measured using the bioreactor. This measurement was confirmed through lyophilization. Measurements of the water content taken using the bioreactor showed a steady increase in water content from 7 to 21 days, initially being less than that of native tissue at 7 and 14 days and eventually increasing to beyond that of native tissue at 21 days, although none of these changes were statistically significant (Fig. 4). According to the measurements obtained using lyophilization, the water content varied very little between all of the time points tested, with no significant change between any of the groups (Fig. 4). The water content at all time points was slightly higher than that of native tissue, as determined through lyophilization.

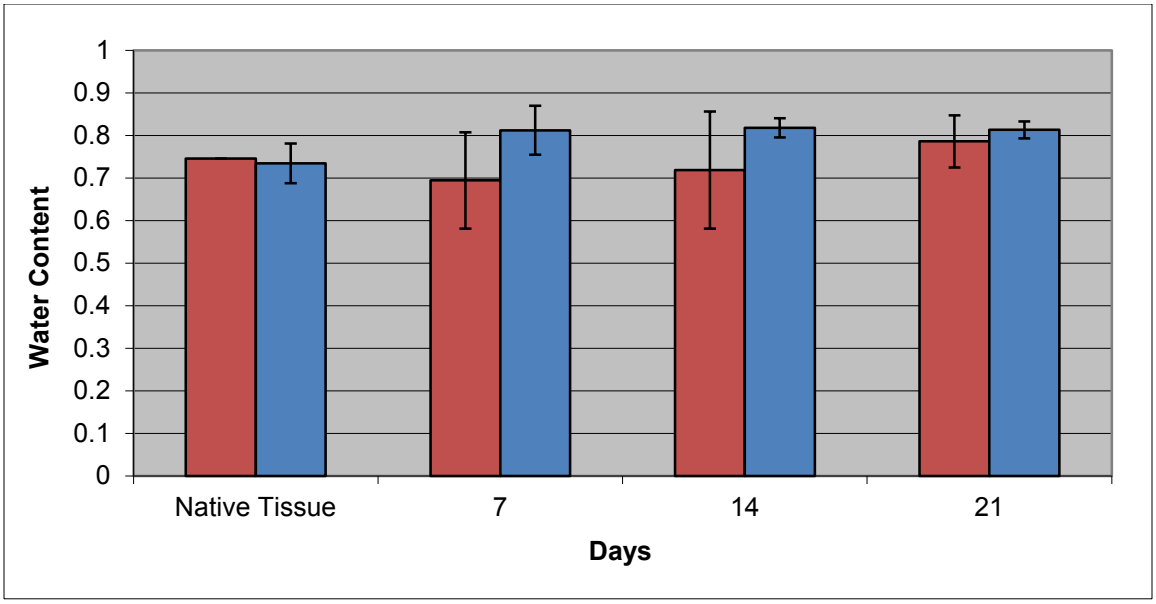

Figure 5. Water content of the constructs as measured by the bioreactor system (■) and by lyophilization (■). Data are shown for native tissue (n=1 for bioreactor and 4 for lyophilization), and at 7 (n=6), 14 (n=6), and 21 days (n=6). Error bars show ±standard deviation.

3.3 Histological Analysis

3.3.1 Live-dead Staining

Transverse sections were obtained from the constructs at pre-determined time intervals (n=4 at each time interval) for live-dead staining with calcein AM and ethidium homodimer (Invitrogen Corp., Carlsbad, CA). Sections were initially visualized from constructs 24 hours after seeding. While there was some evidence of cell death in these scaffolds, the vast majority of cells were viable (Fig. 5). There was evidence of some cells that were present in the center of the constructs; however, there was a superficial layer of cells on both the top and bottom surface of the construct, indicating that many of the cells were present on the surface of the constructs immediately after cell seeding (Fig. 5). This superficial layer was present in all constructs that underwent live-dead staining at 24 hours.

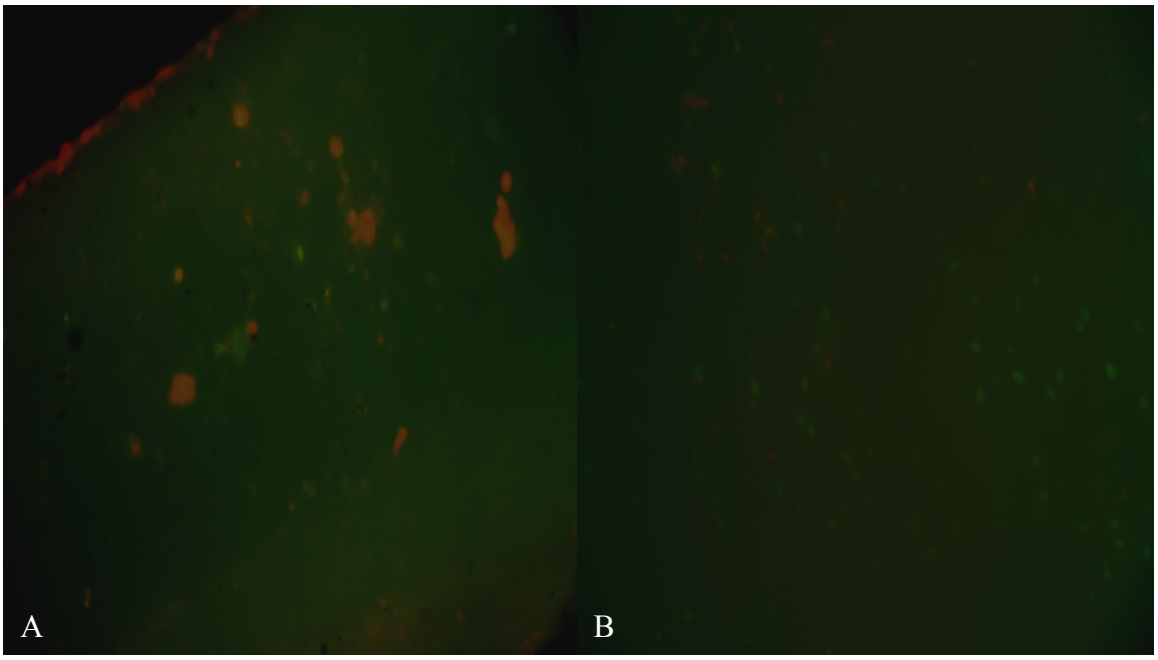

Figure 6. Representative images from constructs 24 hours after cell seeding with either chondrocytes (A) or SHED cells (B) that had undergone live-dead staining. Sections were stained with calcein AM (green, live cells) and ethidium homodimer (red, dead cells).

At 7 days, the majority of cells were again viable, although there were still a number of cells that had died that were still present in the constructs. There was a greater presence of cells distributed throughout the center of the construct at this time point; however, it was still apparent that a large number of the cells were still located in the most superficial layers, and the cell density on the surface of the construct was much higher than in the center (Fig. 6).

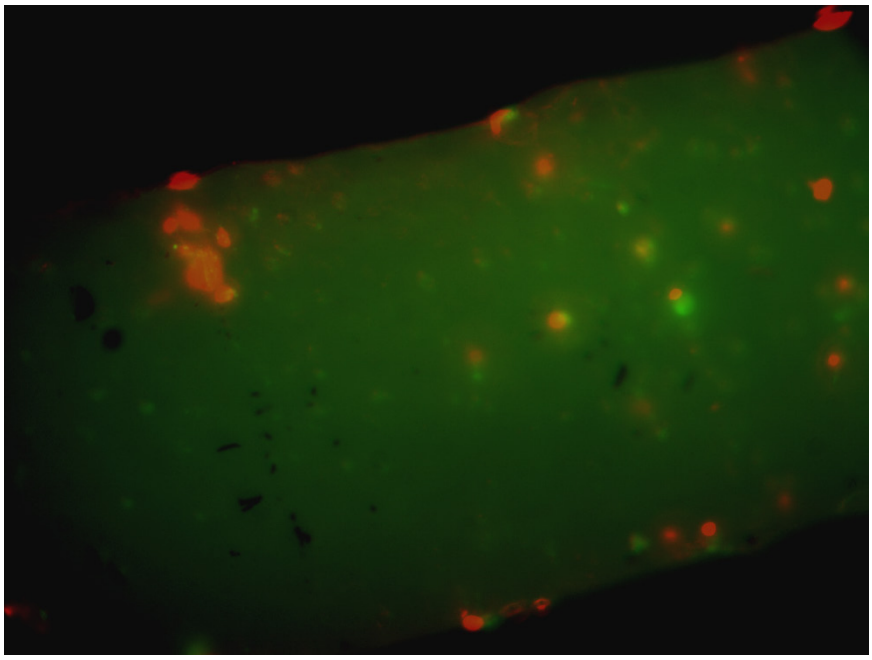

Figure 7. Representative image from constructs 7 days after cell seeding that had undergone live-dead staining. Sections were stained with calcein AM (green, live cells) and ethidium homodimer (red, dead cells).

By 14 days, there was little change in the appearance of live-dead images when compared to those of constructs that were imaged 7 days after cell seeding (Fig. 7). Again, the majority of the cells were viable, and there was some evidence of cell death. Most of the cells that were visible were present on the top and bottom surface of the construct, and there seemed to be little change in the distribution of the cells when compared to constructs from the 24 hours and 7 days after cell seeding groups (Fig. 7).

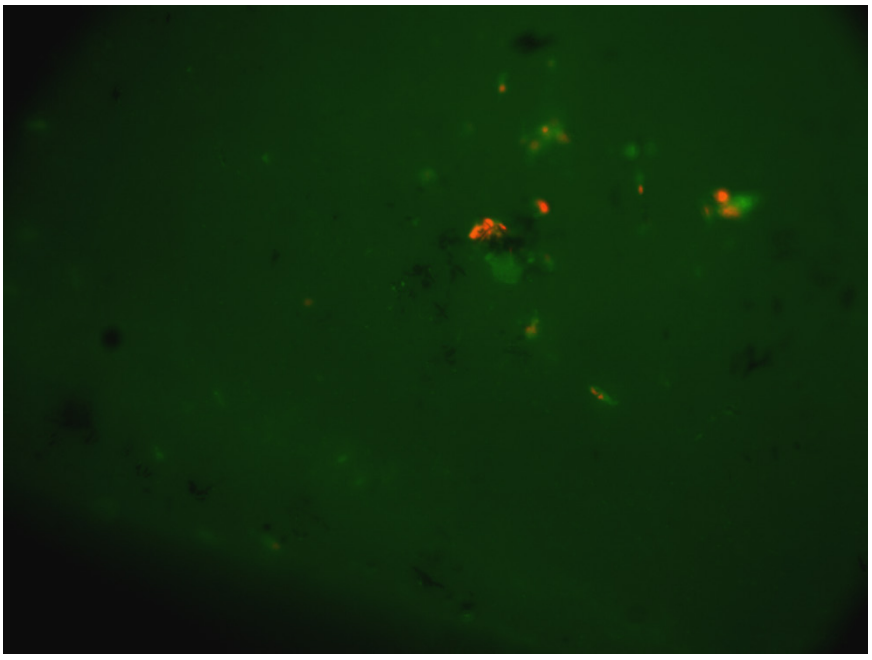

Figure 8. Representative image from constructs 14 days after cell seeding that had undergone live-dead staining. Sections were stained with calcein AM (green, live cells) and ethidium homodimer (red, dead cells).

At 21 days, there was evidence of improved cell distribution throughout the construct (Fig. 8). More cells were visible distributed throughout the center of the construct, but the majority of cells were still found in the superficial regions of the scaffold (Fig. 8). A high level of cell viability was again apparent at this time point; however, with the higher number of cells that were visible, there was a corresponding increase in the number of dead cells that were visualized (Fig. 8). The chondrocytes maintained their round shape at all time points tested, which serves as an indication that the scaffold was able to maintain the phenotype of the loaded chondrocytes.[75]

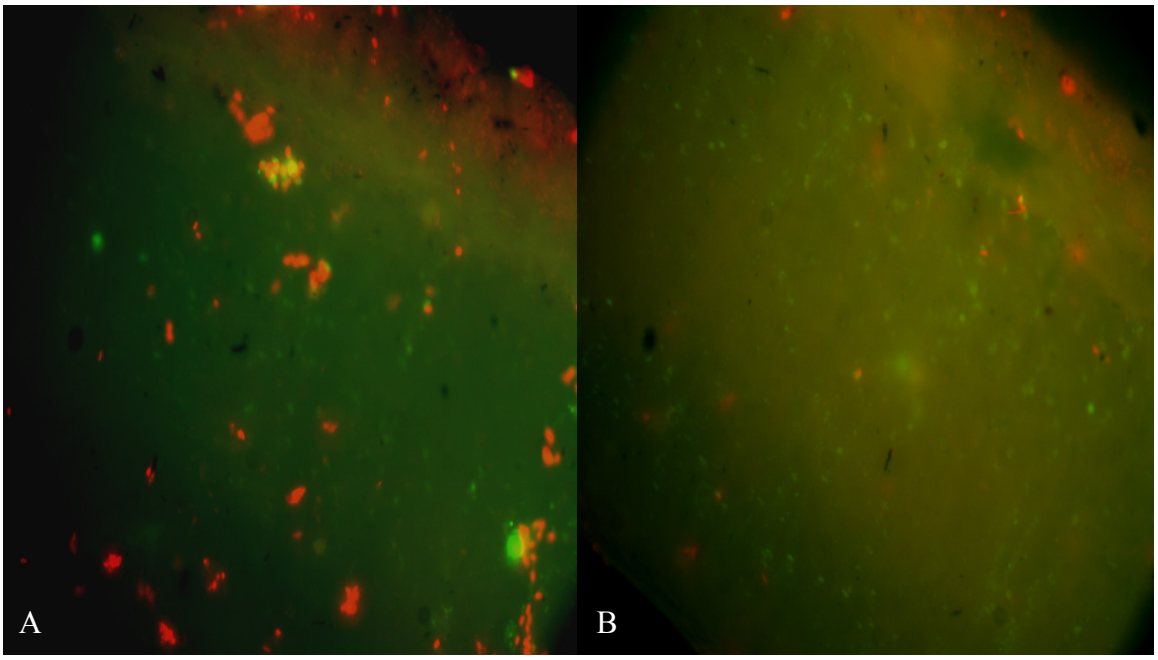

Figure 9. Representative images from constructs 21 days after cell seeding that had undergone live-dead staining. Sections were stained with calcein AM (green, live cells) and ethidium homodimer (red, dead cells).

Live-dead staining of native tissue was performed within about three hours of sacrifice for comparison. Images showed a much higher density of cells found throughout the center of the tissue (Fig. 9). Cellular viability was generally high in these samples, although there was some evidence of cell death in all of the samples (Fig. 9). This was likely due to the fact that the animal had been sacrificed, and the tissue was beginning to become necrotic as a result.

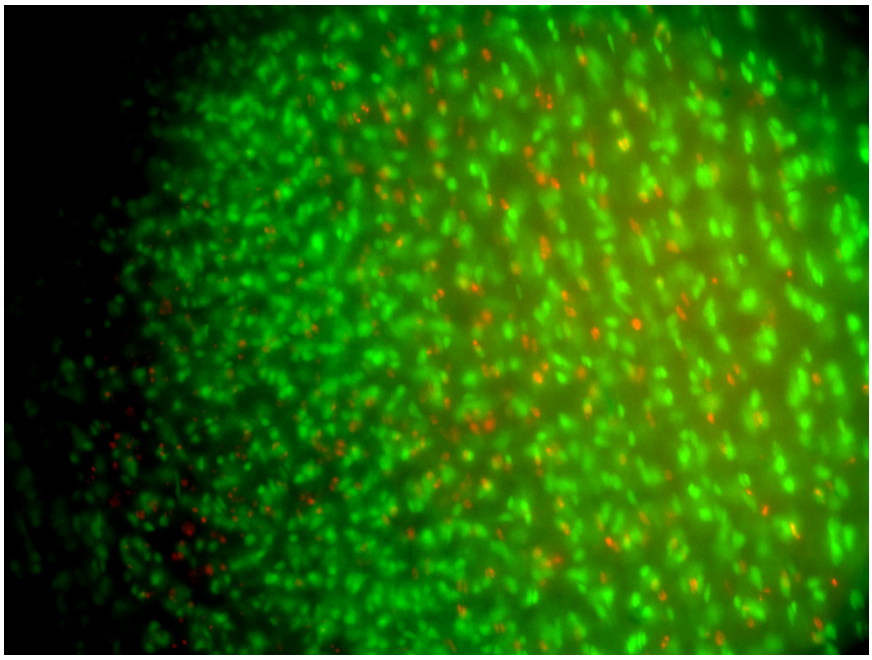

Figure 10. Representative image from native tissue obtained within three hours of animal sacrifice that had undergone live-dead staining. Sections were stained with calcein AM (green, live cells) and ethidium homodimer (red, dead cells).

3.3.2 Hematoxylin and Safranin-O/Eosin Staining

Hematoxylin and Safranin-O or hematoxylin and eosin staining confirmed the results seen using the live-dead staining. Hematoxylin and eosin staining was used for the majority of the constructs, as the PG matrix had not formed to the point that it sufficiently took up the Safranin-O to serve as a counterstain. Twenty-four hours after cell seeding, there were some noticeable cells in the deeper layers of the scaffold. However, there was strong purple staining on the superficial layer of the constructs, which was likely hematoxylin, indicating a large concentration of cell nuclei on the surface of the constructs (Fig. 10). This corroborated what was seen with live-dead staining and suggested that the majority of the cells were located on the outer layers of the scaffold immediately following cell seeding.

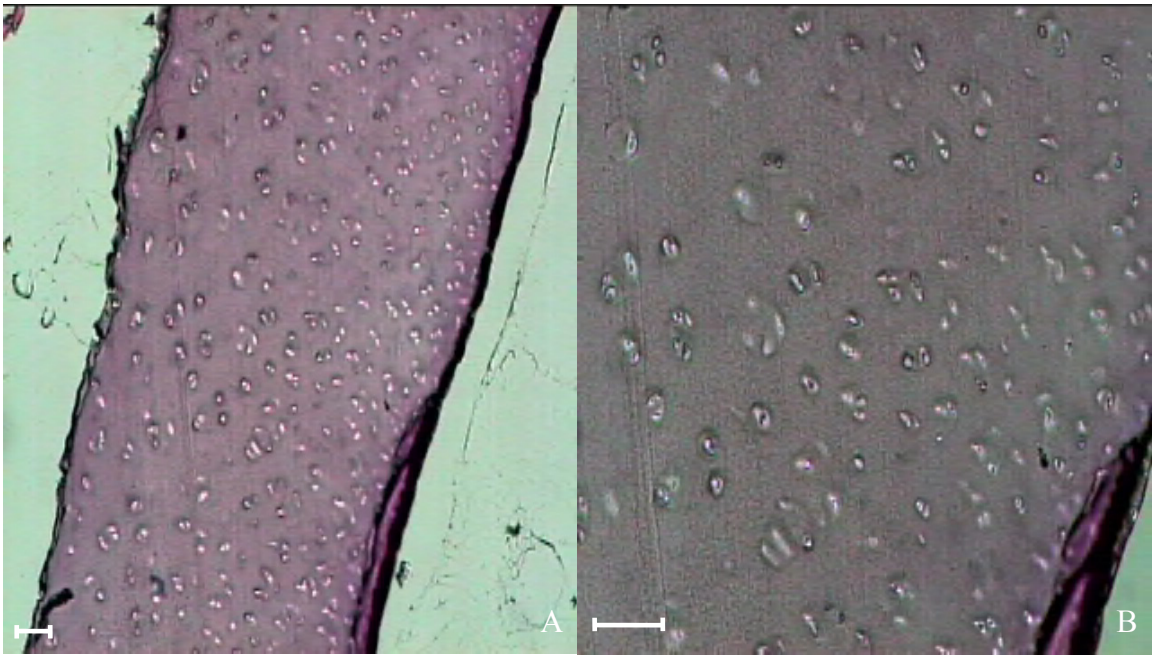

Figure 11. Representative images from hematoxylin and eosin staining of constructs twenty-four hours after cell seeding. Images shown at a magnification of 10x (A) and 20x (B). Scale bars =125 μm (A) and 62.5μm (B).

Constructs imaged at 7 days showed similar heavy hematoxylin staining on the top and bottom layer (Fig. 11). However, better integration into the deeper layers of the scaffold was seen as evidenced by increased nuclei staining throughout the center of the constructs (Fig. 11). Similar to what was seen with the live-dead staining, the majority of the cells remained in the superficial layers of the construct, but there was better cell distribution in the constructs when compared to those constructs imaged at 24 hours.

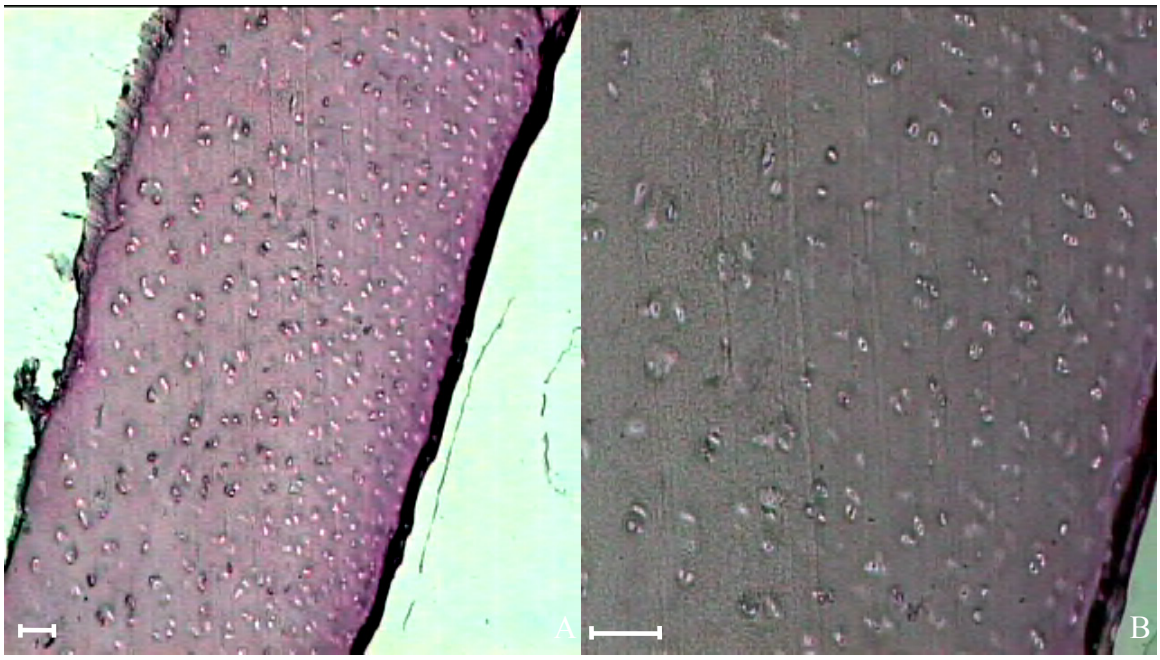

Figure 12. Representative images from hematoxylin and eosin staining of constructs seven days after cell seeding. Images shown at magnification of 10x (A) and 20x (B). Scale bars =125 μm (A) and 62.5μm (B).

By 14 days, further integration of the seeded cells into the scaffolds was seen, as cell nuclei were present at higher levels throughout the construct (Fig. 12). The heavy hematoxylin staining on the superficial layers of the construct had not diminished at this time point, again indicating that the highest concentration of cells was present on the top and bottom layers of the scaffold (Fig. 12). These results confirmed what was seen with live-dead staining.

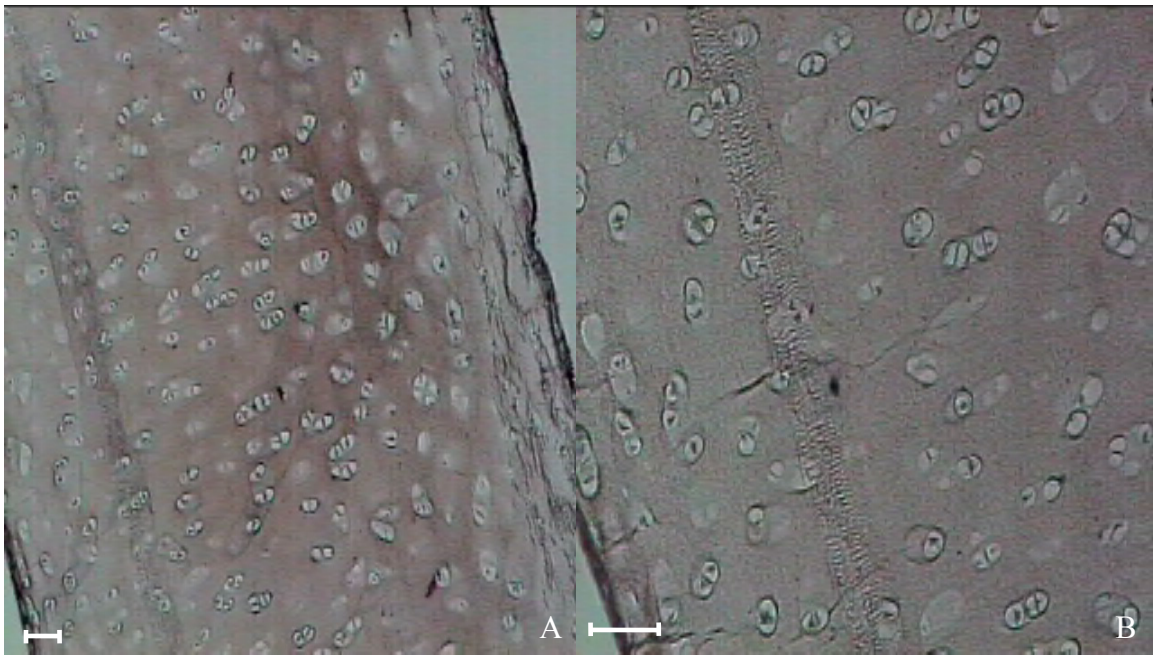

Figure 13. Representative images from hematoxylin and eosin staining of constructs fourteen days after cell seeding. Images shown at magnification of 10x (A) and 20x (B). Scale bars =125 μm (A) and 62.5μm (B).

At 21 days, the highest level of cell integration was seen in the constructs that were imaged. The highest numbers of cell nuclei were seen distributed throughout the center of the scaffold at this time point (Fig. 13). The hematoxylin staining on the superficial layers of the construct was somewhat diminished; however, there was still an indication that the majority of the cells were on the outer layers of the construct (Fig. 13). These results were similar to those seen during live-dead staining.

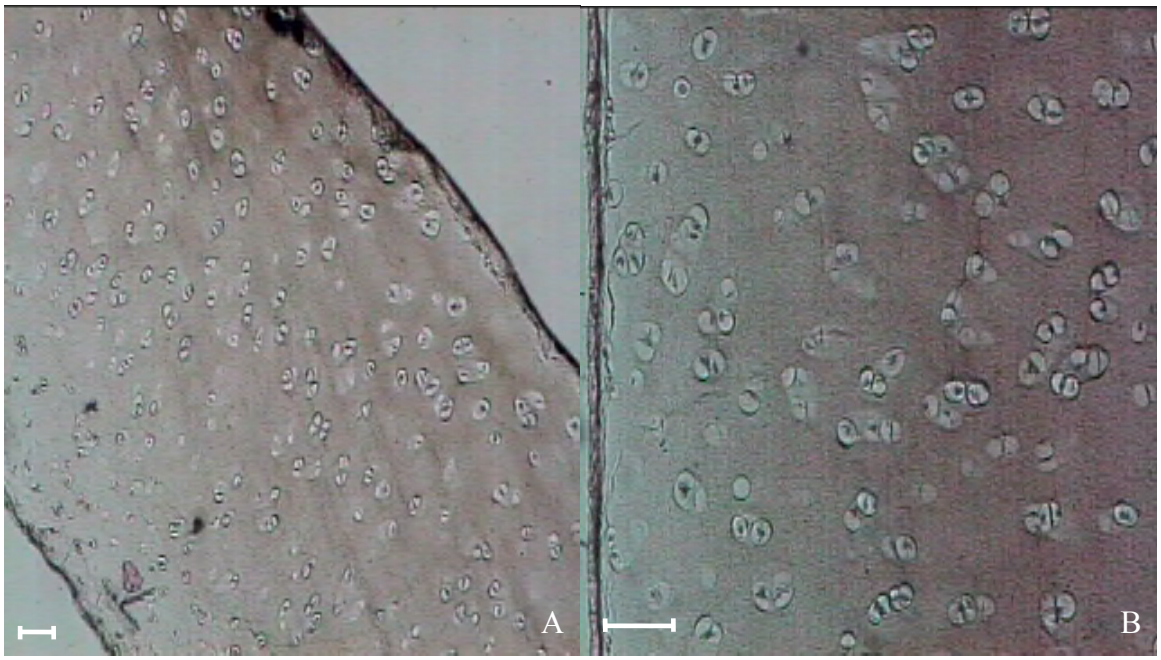

Figure 14. Representative images from hematoxylin and eosin staining of constructs twenty-one days after cell seeding. Images shown at a magnification of 10x (A) and 20x (B). Scale bars =125 μm (A) and 62.5μm (B).

3.3.3 DNA Quantification

Cell concentration measurements of the cell solution taken during cell seeding indicated that a large number of the cells that were used to seed the scaffold were retained by the scaffold during seeding. Further cell concentration measurements of the medium used to supplement the constructs during culture were generally low or undetectable, indicating that the cells were able to attach to the scaffold and remain within the scaffold after cell seeding. DNA quantification performed 24 hours after cell seeding showed that a relatively high cell seeding efficiency (54.1±3.63%, n=3), as well as a high cell density (14,518±750 cells/mg, n=3) compared to that of native tissue (6,103±793 cells/mg) was achieved using the centrifugation loading method. The number of cells in the constructs steadily increased to over 4 million at 21 days (n=6), well above the number of cells found in native tissue (Fig. 14). Also, although the number of cells in the scaffold

continued to increase at both 7 and 14 days after cell seeding, the sharpest increase in the cell number was found in the constructs 21 days after seeding, mirroring the trend that was observed when measuring the PG accumulation in the constructs (Fig. 14).

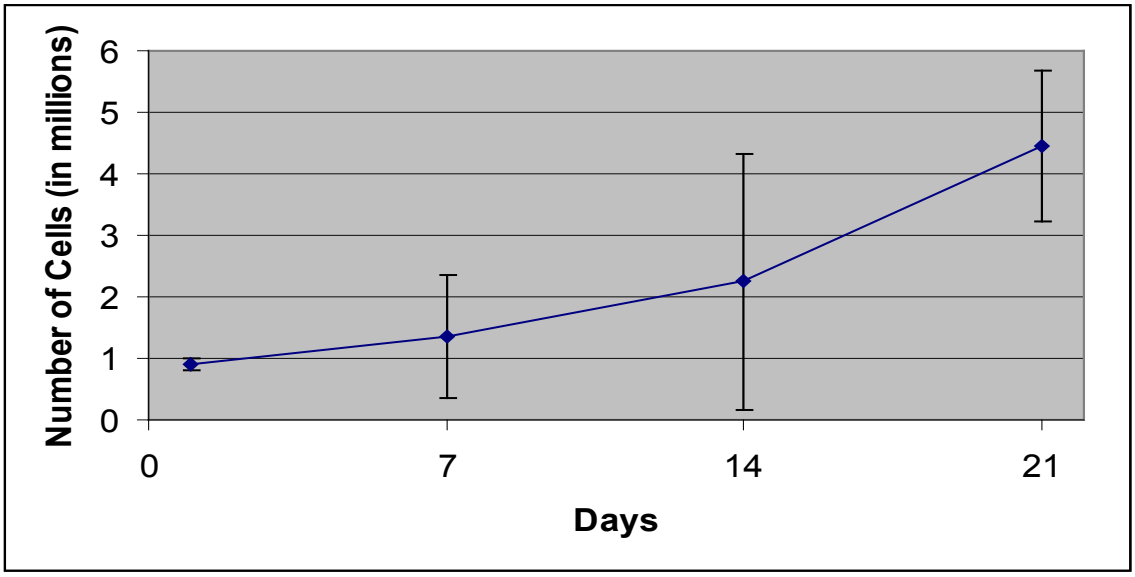

Figure 15. Number of cells in the constructs as measured through DNA quantification. Data are shown at 24 hours (n=3), 7 (n=4), 14 (n=4), and 21 days (n=6) after cell seeding. Error bars show ±standard deviation.

CHAPTER 4: DISCUSSION

4.1 Preliminary Measurements

DNA and DMMB quantification showed that the scaffolds were decellularized and that the PG had been removed before they were recellularized. This was confirmed through hematoxylin and Safranin-O staining (Fig. 1), indicating that the samples were free of cells and suitable for use as a scaffold for tissue engineering and that any PG that was present in the scaffold at the designated time intervals was deposited by the seeded chondrocytes.

4.2 Bioreactor Measurements

Measurements taken using the bioreactor and the DMMB assay indicated that the scaffold encouraged ECM deposition by the seeded chondrocytes. The increase in PG accumulation at each time point up to 21 days suggests that the scaffold is able to effectively recapitulate the *in vivo* environment of the chondrocytes, and the PG accumulation could be expected to increase at time points beyond those tested. There was also a rapid increase in the PG accumulation from 14 days to 21 days. This could be due to the fact that it took the cells some time to recover from the somewhat stressful seeding process, and at 21 days, they had fully recovered and had begun to produce PG at a much faster rate. However, there are other factors that could have led to this sharp increase in PG accumulation that will be discussed later. There was a corresponding decrease in the hydraulic permeability in response to the increase in fixed charge density (Fig. 2). This result was anticipated, as the hydraulic permeability decreases as the fixed charge density increases.[76] Therefore, the dramatic decrease in hydraulic permeability at 21 days was expected in response to the significant increase in FCD at 21 days. The small increase in

FCD seen at 7 and 14 days was likely not significant enough to produce a measurable change in hydraulic permeability, which could account for why there was little change in the hydraulic permeability from baseline at 7 and 14 days despite an increase in the PG accumulation.

Overall, the PG accumulation failed to reach native levels, only achieving about 30% of the FCD of native tissue at 21 days. This is likely a consequence of the culture conditions of the tissue engineered constructs after cell seeding.[77] While chondrocytes will naturally produce PG when left in static culture, especially when they are seeded in a scaffold that attempts to recapitulate their *in vivo* environment, ECM deposition occurs at a much higher rate when some other stimulus is provided to the cells.[77,78] Dynamic mechanical loading, flow-perfusion, continuous culture, and treatment with various factors have all been shown to upregulate ECM production by cells seeded in tissue engineered constructs *in vitro*.[79-84] While the PG accumulation within the construct could be expected to continue to increase, even to native levels with enough time in culture, using one of these methods could serve to increase the PG production rate of the seeded chondrocytes in an attempt to reach native PG levels within 2-3 weeks of culture. This would provide a more optimal outcome, as a shorter culture time is more desirable for clinical applications. Just as with the FCD, the hydraulic permeability of the tissue engineered constructs did not reach the measured hydraulic permeability of native tissue. However, since FCD and hydraulic permeability are directly related[70], it is expected that with a continued increase in FCD the hydraulic permeability would decrease to a value that is closer to that of native tissue.

The water content measurements taken using the bioreactor and through lyophilization differed from one another slightly, in that the measurements taken using the bioreactor showed a slight increase in water content from baseline up to 21 days, while the measurements obtained using lyophilization showed very little change in the water content of the constructs between any of the time points tested. The difference between the two measurements likely stems from the fact that the water content as measured through lyophilization is calculated using Equation 7, which is based on the assumption that the ratio of the density of water to the density of tissue is 1. This, of course, is not a completely accurate assumption and likely explains why the two measurements differ from one another. Despite this possible discrepancy, both of these results were unexpected given the increase in FCD over time. It is expected that, as FCD increases, water content will in turn decrease, as the PG take up more volume within the tissue leaving less empty space for water to diffuse into the tissue.[70] The opposite was seen in this study, as the water content either increased or stayed the same with increased FCD depending on which measurement was used for analysis. This finding could be explained by the function of PG within cartilagionous tissues. PG is a negatively charged extracellular matrix protein that, among other things, allows tissues such as cartilage to retain water.[85] This allows cartilage to swell in an uncompressed state and also affords it the osmotic resistance that is necessary to withstand compression. In this experiment, the PG accumulation in the constructs at the later time points could have caused the tissue to swell, thereby increasing the water content within the tissue. This increase in water diffusing into the tissue as it swelled could have offset the increased tissue volume that

was occupied by the accumulated PG, which would explain why the water content increased or remained the same despite the increase in PG accumulation.

4.3 Histological Analysis

Live-dead staining showed that the scaffold was capable of supporting cell viability at all time points tested. While there were some dead cells visible at all time points, the vast majority of cells were viable. DNA measurements corroborated these findings, as the cells continued to proliferate up to 21 days to over four times the initial number of cells seeded within the scaffolds. Additionally, although there was some cell death at 24 hours, most of the cells were viable, indicating that the chondrocytes were capable of withstanding the centrifugation cell seeding technique. Images taken during live-dead staining indicated that the majority of the cells remained on the superficial layer of the constructs at all time points. However, at 21 days, there seemed to be higher integration of the cells into the center of the constructs. The mechanism for this increased level of cell integration into the center of the constructs is unknown at this time. The cartilage ECM has an extremely low porosity, with pore sizes much smaller than the reported spherical diameter of chondrocytes.[1,86] Therefore, it was surprising to find that the chondrocytes seemed to be able to move deeper into the scaffold after they were seeded mainly in the superficial layers. More testing is needed to elucidate the mechanism by which the chondrocytes were able to move deeper into the scaffold over time. Even at 21 days, the distribution throughout the constructs was not comparable to that of native tissue, as the cell density in the deeper regions of native tissue was visibly higher than in the constructs. These findings were confirmed through hematoxylin and eosin staining and hematoxylin and Safranin-O staining. Similar distribution was seen as

that observed during live-dead staining, with the best distribution occurring in the constructs at 14 and 21 days after cell seeding. Again, the cellular distribution was not as uniform as that seen in native tissue even at 21 days.

While the scaffold was expected to encourage cell viability due to its similarity to native tissue, the high level of cell proliferation was a somewhat unexpected result obtained in this study. Fully differentiated chondrocytes do not typically exhibit high levels of proliferation in their *in vivo* environment.[3] This is due to the extremely dense nature of the surrounding tissue, which restricts them from entering a proliferative pathway. The initial concentration of the cell solution used to seed the scaffolds was chosen with this fact in mind and was designed so that enough cells would be seeded within the scaffold to mimic the cell density of native tissue without the need for cell proliferation. It was not anticipated that the seeded chondrocytes would proliferate at all, much less at such a high rate. The reason for this high rate of proliferation may be explained by the cell distribution within the scaffold. Since the majority of the cells remained in the superficial regions of the scaffold, they did not experience the typical environmental cues that are received by chondrocytes *in vivo* that restrict them from undergoing mitosis. The chondrocytes that were in the superficial regions of the scaffold most likely continued to proliferate throughout the study because of the lack of these environmental cues.

Although a high cell seeding efficiency and cell density compared to native tissue was achieved using the centrifugation loading method, the distribution of the cells within the constructs did not mirror that of native tissue as closely as was anticipated. This was likely due to the lack of an interconnected pore structure within the scaffolds. In its native

form, cartilage has a very poorly interconnected porous system.[87] This limits cell movement within the tissue, as the cells do not have well-developed routes of transport. In this study, the PG component of the ECM was removed to create scaffolds in an attempt to create pores through which the cells could be seeded within the tissue. While the number of cells that were present in the center of the constructs seemed to increase over time, a more defined pore structure may be needed to achieve the cell distribution observed in native tissue. Furthermore, nutrient diffusion limitations through the constructs could have prevented the cells from moving deeper into the scaffolds. As discussed above, articular cartilage is extremely dense, and nutrient diffusion is very slow through the tissue.[88] The constructs were left in static culture, so all nutrient transport occurred through diffusion. Nutrient levels would have been much higher in the superficial zones of the construct, which could have discouraged the cells from migrating deeper within the scaffold.

4.4 Conclusions

In summary, this study investigated the tissue engineering potential of a decellularized porcine scaffold in which the PG had also been removed. A novel cell seeding technique incorporating centrifugation was used to increase the cell seeding efficiency and cell density of tissue engineered constructs and to improve the cellular distribution within the scaffold. The scaffold promoted cell viability and proliferation and encouraged ECM deposition. Furthermore, the novel cell seeding technique improved cell seeding efficiency and proved capable of achieving a cell density comparable to that of native tissue. However, cell distribution within the scaffolds was mostly confined to the superficial layers of the scaffold, and cells were not as equally distributed throughout

as compared to native tissue. Overall, this study demonstrated that the scaffold could have a potential use in cartilage tissue engineering. Future studies should seek to use novel cell seeding methods to improve the cell distribution within the scaffold. Also, different culture methods should be employed to increase the PG production rate.

4.5 Limitations of the Current Study

The primary limitation of this study is the lack of mechanical testing that could be used to help characterize the functional capabilities of the tissue engineered constructs. One of the principal functions of cartilage within the body is to provide cushioning and mechanical support to the joints.[87] To accomplish this, a certain level of mechanical strength is necessary. The extensive collagen network is responsible for the majority of cartilage's mechanical strength[89], and since the collagen network was not compromised during the decellularization and removal of PG, there should not be a significant change in the mechanical strength of the scaffolds. However, as mentioned above, PG does provide some mechanical support by allowing cartilage to resist compressive loads through water retention.[85] Therefore, the mechanical strength of the scaffolds could be less than that of native tissue. Mechanical testing could provide the means to characterize how much mechanical strength is lost during the digestion process used to create the scaffolds and could also be used to determine whether or not the mechanical strength increases to native levels as the seeded cells deposit ECM. Future studies should incorporate the use of mechanical testing to further characterize the functional properties of the tissue engineered constructs.

4.6 Future Studies

Currently, studies are underway that are seeking novel cell seeding techniques that can improve cellular distribution within the constructs. Direct injection of the cells into the scaffold and further modifications to the scaffold before seeding, such as treatment of the scaffold with collagenase for short periods of time and creating tiny punctures in the scaffold, have all been sought as a means to accomplish this. In a recent study, investigators cut decellularized cartilage into very thin sheets and then stacked the sheets pipetting a cell solution onto each sheet as it was added to create a tissue engineered construct.[61] Using this technique, the authors achieved improved cellular distribution throughout the construct and found that cartilage-like tissue had developed at 12 weeks. A similar technique has been employed in our most recent studies. Cartilage tissue samples are prepared in 50 micrometer thick sheets. The sheets are then stacked one on top of the other with 5 microliters of cell solution added to the top of each sheet. The larger cylindrical piece of the novel cell seeding device is used for support during cell seeding, which has allowed 20 cell sheets to be stacked together to achieve a height of 1 millimeter. Live-dead staining has indicated that improved cell distribution throughout the construct has been achieved using this method to seed SHED cells. In a future study, chondrocytes will be used to determine the ability of the scaffold to recapitulate itself as a solid piece of tissue and achieve the properties of native cartilage in long-term culture. Once a suitable tissue engineered construct has been developed *in vitro*, *in vivo* studies will be necessary to determine the immunogenicity of the construct.

References

1 Buckwalter, J. A., Mankin, H. J. & Grodzinsky, A. J. Articular cartilage and osteoarthritis. *Instructional course lectures* **54**, 465-480 (2005).

2 Huber, M., Trattnig, S. & Lintner, F. Anatomy, biochemistry, and physiology of articular cartilage. *Investigative radiology* **35**, 573-580 (2000).

3 Poole, A. R. *et al.* Composition and structure of articular cartilage: a template for tissue repair. *Clinical orthopaedics and related research*, S26-33 (2001).

4 Bijlsma, J. W., Berenbaum, F. & Lafeber, F. P. Osteoarthritis: an update with relevance for clinical practice. *Lancet* **377**, 2115-2126, doi:10.1016/S0140-6736(11)60243-2 (2011).

5 Hunter, D. J. & Lo, G. H. The management of osteoarthritis: an overview and call to appropriate conservative treatment. *The Medical clinics of North America* **93**, 127-143, xi, doi:10.1016/j.mcna.2008.07.009 (2009).

6 Helmick, C. G. *et al.* Estimates of the prevalence of arthritis and other rheumatic conditions in the United States. Part I. *Arthritis and rheumatism* **58**, 15-25, doi:10.1002/art.23177 (2008).

7 National and state medical expenditures and lost earnings attributable to arthritis and other rheumatic conditions--United States, 2003. *MMWR. Morbidity and mortality weekly report* **56**, 4-7 (2007).

8 Walker, J. Effective management strategies for osteoarthritis. *Br J Nurs* **20**, 81-85 (2011).

9 Williams, R. J., 3rd & Harnly, H. W. Microfracture: indications, technique, and results. *Instructional course lectures* **56**, 419-428 (2007).

10 Sarzi-Puttini, P. *et al.* Osteoarthritis: an overview of the disease and its treatment strategies. *Seminars in arthritis and rheumatism* **35**, 1-10, doi:10.1016/j.semarthrit.2005.01.013 (2005).

11 Moreira-Teixeira, L. S., Georgi, N., Leijten, J., Wu, L. & Karperien, M. Cartilage tissue engineering. *Endocrine development* **21**, 102-115, doi:10.1159/000328140 (2011).

12 Hunziker, E. Quantitative structural organization of normal adult human articular cartilage. *Osteoarthritis and Cartilage* **10**, 564-572, doi:10.1053/joca.2002.0814 (2002).

13 Heinegard, D. & Saxne, T. The role of the cartilage matrix in osteoarthritis. *Nature reviews. Rheumatology* **7**, 50-56, doi:10.1038/nrrheum.2010.198 (2011).

14 Nelson, T. J., Behfar, A., Yamada, S., Martinez-Fernandez, A. & Terzic, A. Stem cell platforms for regenerative medicine. *Clinical and translational science* **2**, 222-227, doi:10.1111/j.1752-8062.2009.00096.x (2009).

15 Hardingham, T. E., Rayan, V. & Lewthwaite, J. C. [Regulation of cartilage matrix synthesis by chondrocytes]. *Rev Rhum Ed Fr* **61**, 93S-98S (1994).

16 Jackson, A. & Gu, W. Transport Properties of Cartilaginous Tissues. *Current rheumatology reviews* **5**, 40, doi:10.2174/157339709787315320 (2009).

17 Mistry, D., Oue, Y., Chambers, M. G., Kayser, M. V. & Mason, R. M. Chondrocyte death during murine osteoarthritis. *Osteoarthritis and cartilage / OARS, Osteoarthritis Research Society* **12**, 131-141 (2004).

18 Martel-Pelletier, J., Boileau, C., Pelletier, J. P. & Roughley, P. J. Cartilage in normal and osteoarthritis conditions. *Best practice & research. Clinical rheumatology* **22**, 351-384, doi:10.1016/j.berh.2008.02.001 (2008).

19 Wang, J., Verdonk, P., Elewaut, D., Veys, E. M. & Verbruggen, G. Homeostasis of the extracellular matrix of normal and osteoarthritic human articular cartilage chondrocytes in vitro. *Osteoarthritis and cartilage / OARS, Osteoarthritis Research Society* **11**, 801-809 (2003).

20 Nesic, D. *et al.* Cartilage tissue engineering for degenerative joint disease. *Advanced drug delivery reviews* **58**, 300-322, doi:10.1016/j.addr.2006.01.012 (2006).

21 Nunes, S. S., Song, H., Chiang, C. K. & Radisic, M. Stem cell-based cardiac tissue engineering. *Journal of cardiovascular translational research* **4**, 592-602, doi:10.1007/s12265-011-9307-x (2011).

22 Willerth, S. M. Neural tissue engineering using embryonic and induced pluripotent stem cells. *Stem cell research & therapy* **2**, 17, doi:10.1186/scrt58 (2011).

23 Harris, J. D., Siston, R. A., Pan, X. & Flanigan, D. C. Autologous chondrocyte implantation: a systematic review. *The Journal of bone and joint surgery. American volume* **92**, 2220-2233, doi:10.2106/JBJS.J.00049 (2010).

24 Harris, J. D. *et al.* Failures, re-operations, and complications after autologous chondrocyte implantation--a systematic review. *Osteoarthritis and cartilage / OARS, Osteoarthritis Research Society* **19**, 779-791, doi:10.1016/j.joca.2011.02.010 (2011).

25 Keeney, M., Lai, J. H. & Yang, F. Recent progress in cartilage tissue engineering. *Current opinion in biotechnology* **22**, 734-740, doi:10.1016/j.copbio.2011.04.003 (2011).

26 Gloria, A., De Santis, R. & Ambrosio, L. Polymer-based composite scaffolds for tissue engineering. *Journal of applied biomaterials & biomechanics : JABB* **8**, 57-67 (2010).

27 Liang, W. H. *et al.* Concentrated collagen-chondroitin sulfate scaffolds for tissue engineering applications. *Journal of biomedical materials research. Part A* **94**, 1050-1060, doi:10.1002/jbm.a.32774 (2010).

28 Toh, W. S., Spector, M., Lee, E. H. & Cao, T. Biomaterial-mediated delivery of microenvironmental cues for repair and regeneration of articular cartilage. *Molecular pharmaceutics* **8**, 994-1001, doi:10.1021/mp100437a (2011).

29 Stoddart, M. J., Grad, S., Eglin, D. & Alini, M. Cells and biomaterials in cartilage tissue engineering. *Regenerative medicine* **4**, 81-98, doi:10.2217/17460751.4.1.81 (2009).

30 Spiller, K. L., Holloway, J. L., Gribb, M. E. & Lowman, A. M. Design of semi-degradable hydrogels based on poly(vinyl alcohol) and poly(lactic-co-glycolic acid) for cartilage tissue engineering. *Journal of tissue engineering and regenerative medicine* **5**, 636-647, doi:10.1002/term.356 (2011).

31 Swieszkowski, W., Tuan, B. H., Kurzydlowski, K. J. & Hutmacher, D. W. Repair and regeneration of osteochondral defects in the articular joints. *Biomolecular engineering* **24**, 489-495, doi:10.1016/j.bioeng.2007.07.014 (2007).

32 Zhang, C. *et al.* Oligo(trimethylene carbonate)-poly(ethylene glycol)-oligo(trimethylene carbonate) triblock-based hydrogels for cartilage tissue engineering. *Acta biomaterialia* **7**, 3362-3369, doi:10.1016/j.actbio.2011.05.024 (2011).

33 Hsieh, W. C., Chang, C. P. & Lin, S. M. Morphology and characterization of 3D micro-porous structured chitosan scaffolds for tissue engineering. *Colloids and surfaces. B, Biointerfaces* **57**, 250-255, doi:10.1016/j.colsurfb.2007.02.004 (2007).

34 Kim, I. L., Mauck, R. L. & Burdick, J. A. Hydrogel design for cartilage tissue engineering: a case study with hyaluronic acid. *Biomaterials* **32**, 8771-8782, doi:10.1016/j.biomaterials.2011.08.073 (2011).

35 Malda, J. *et al.* The effect of PEGT/PBT scaffold architecture on the composition of tissue engineered cartilage. *Biomaterials* **26**, 63-72, doi:10.1016/j.biomaterials.2004.02.046 (2005).

36 Woodfield, T. B. *et al.* Rapid prototyping of anatomically shaped, tissue-engineered implants for restoring congruent articulating surfaces in small joints. *Cell proliferation* **42**, 485-497, doi:10.1111/j.1365-2184.2009.00608.x (2009).

37 Mouthuy, P. A., Ye, H., Triffitt, J., Oommen, G. & Cui, Z. Physico-chemical characterization of functional electrospun scaffolds for bone and cartilage tissue engineering. *Proceedings of the Institution of Mechanical Engineers. Part H, Journal of engineering in medicine* **224**, 1401-1414 (2010).

38 Bi, L. *et al.* Effects of different cross-linking conditions on the properties of genipin-cross-linked chitosan/collagen scaffolds for cartilage tissue engineering. *Journal of materials science. Materials in medicine* **22**, 51-62, doi:10.1007/s10856-010-4177-3 (2011).

39 Hollister, S. J. Porous scaffold design for tissue engineering. *Nature materials* **4**, 518-524, doi:10.1038/nmat1421 (2005).

40 Spiller, K. L., Maher, S. A. & Lowman, A. M. Hydrogels for the repair of articular cartilage defects. *Tissue engineering. Part B, Reviews* **17**, 281-299, doi:10.1089/ten.TEB.2011.0077 (2011).

41 Klein, T. J., Malda, J., Sah, R. L. & Hutmacher, D. W. Tissue engineering of articular cartilage with biomimetic zones. *Tissue engineering. Part B, Reviews* **15**, 143-157, doi:10.1089/ten.TEB.2008.0563 (2009).

42 Yang, Z. *et al.* Fabrication and repair of cartilage defects with a novel acellular cartilage matrix scaffold. *Tissue engineering. Part C, Methods* **16**, 865-876, doi:10.1089/ten.TEC.2009.0444 (2010).

43 Toolan, B. C., Frenkel, S. R., Pereira, D. S. & Alexander, H. Development of a novel osteochondral graft for cartilage repair. *Journal of biomedical materials research* **41**, 244-250 (1998).

44 Kheir, E. *et al.* Development and characterization of an acellular porcine cartilage bone matrix for use in tissue engineering. *Journal of biomedical materials research. Part A* **99**, 283-294, doi:10.1002/jbm.a.33171 (2011).

45 Yang, Q. *et al.* A cartilage ECM-derived 3-D porous acellular matrix scaffold for in vivo cartilage tissue engineering with PKH26-labeled chondrogenic bone marrow-derived mesenchymal stem cells. *Biomaterials* **29**, 2378-2387, doi:10.1016/j.biomaterials.2008.01.037 (2008).

46 Ng, R., Gurm, J. S. & Yang, S. T. Centrifugal seeding of mammalian cells in nonwoven fibrous matrices. *Biotechnol Prog* **26**, 239-245, doi:10.1002/btpr.317 (2010).

47 Shahin, K. & Doran, P. M. Improved seeding of chondrocytes into polyglycolic acid scaffolds using semi-static and alginate loading methods. *Biotechnology Progress* **27**, 191-200, doi:10.1002/btpr.509 (2011).

48 Weinand, C., Xu, J. W., Peretti, G. M., Bonassar, L. J. & Gill, T. J. Conditions affecting cell seeding onto three-dimensional scaffolds for cellular-based

biodegradable implants. *Journal of biomedical materials research. Part B, Applied biomaterials* **91**, 80-87, doi:10.1002/jbm.b.31376 (2009).

49 Li, W. J., Jiang, Y. J. & Tuan, R. S. Cell-nanofiber-based cartilage tissue engineering using improved cell seeding, growth factor, and bioreactor technologies. *Tissue engineering. Part A* **14**, 639-648, doi:10.1089/tea.2007.0136 (2008).

50 Han, E., Chen, S. S., Klisch, S. M. & Sah, R. L. Contribution of proteoglycan osmotic swelling pressure to the compressive properties of articular cartilage. *Biophysical journal* **101**, 916-924, doi:10.1016/j.bpj.2011.07.006 (2011).

51 Responte, D. J., Natoli, R. M. & Athanasiou, K. A. Collagens of articular cartilage: structure, function, and importance in tissue engineering. *Critical reviews in biomedical engineering* **35**, 363-411 (2007).

52 Bastiaansen-Jenniskens, Y. M. *et al.* Contribution of collagen network features to functional properties of engineered cartilage. *Osteoarthritis and cartilage / OARS, Osteoarthritis Research Society* **16**, 359-366, doi:10.1016/j.joca.2007.07.003 (2008).

53 Bassleer, C., Gysen, P., Foidart, J. M., Bassleer, R. & Franchimont, P. Human chondrocytes in tridimensional culture. *In vitro cellular & developmental biology : journal of the Tissue Culture Association* **22**, 113-119 (1986).

54 Bosnakovski, D. *et al.* Chondrogenic differentiation of bovine bone marrow mesenchymal stem cells (MSCs) in different hydrogels: influence of collagen type II extracellular matrix on MSC chondrogenesis. *Biotechnology and bioengineering* **93**, 1152-1163, doi:10.1002/bit.20828 (2006).

55 Buckwalter, J. A. & Mankin, H. J. Articular cartilage: tissue design and chondrocyte-matrix interactions. *Instructional course lectures* **47**, 477-486 (1998).

56 Chiu, L.-H. *et al.* Differential effect of ECM molecules on re-expression of cartilaginous markers in near quiescent human chondrocytes. *Journal of Cellular Physiology* **226**, 1981-1988, doi:10.1002/jcp.22530 (2011).

57 Wong, M., Wuethrich, P., Eggli, P. & Hunziker, E. Zone-specific cell biosynthetic activity in mature bovine articular cartilage: a new method using confocal microscopic stereology and quantitative autoradiography. *Journal of orthopaedic research : official publication of the Orthopaedic Research Society* **14**, 424-432, doi:10.1002/jor.1100140313 (1996).

58 Zheng, L. *et al.* Chondrogenic differentiation of mesenchymal stem cells induced by collagen-based hydrogel: an in vivo study. *Journal of biomedical materials research. Part A* **93**, 783-792, doi:10.1002/jbm.a.32588 (2010).

59 von der Mark K, G. V., von der Mark H, Muller P. Relationship between cell shape and type of collagen synthesized as chondrocytes lose their cartilage phenotype in culture. *Nature* **266**, 531-532 (1977).

60 Pei, M., Li, J. T., Shoukry, M. & Zhang, Y. A review of decellularized stem cell matrix: a novel cell expansion system for cartilage tissue engineering. *European cells & materials* **22**, 333-343; discussion 343 (2011).

61 Gong, Y. Y. *et al.* A sandwich model for engineering cartilage with acellular cartilage sheets and chondrocytes. *Biomaterials* **32**, 2265-2273, doi:10.1016/j.biomaterials.2010.11.078 (2011).

62 Villalona, G. A. *et al.* Cell-seeding techniques in vascular tissue engineering. *Tissue engineering. Part B, Reviews* **16**, 341-350, doi:10.1089/ten.TEB.2009.0527 (2010).

63 Francioli, S. E. *et al.* Effect of three-dimensional expansion and cell seeding density on the cartilage-forming capacity of human articular chondrocytes in type II collagen sponges. *Journal of biomedical materials research. Part A* **95**, 924-931, doi:10.1002/jbm.a.32917 (2010).

64 Talukdar, S., Nguyen, Q. T., Chen, A. C., Sah, R. L. & Kundu, S. C. Effect of initial cell seeding density on 3D-engineered silk fibroin scaffolds for articular cartilage tissue engineering. *Biomaterials* **32**, 8927-8937, doi:10.1016/j.biomaterials.2011.08.027 (2011).

65 Beloti, M. M., Tambasco De Oliveira, P., Perri De Carvalho, P. S. & Rosa, A. L. Seeding osteoblastic cells into a macroporous biodegradable CaP/PLGA scaffold by a centrifugal force. *Journal of biomaterials applications* **23**, 481-495, doi:10.1177/0885328208094082 (2009).

66 Dai, W., Dong, J., Chen, G. & Uemura, T. Application of low-pressure cell seeding system in tissue engineering. *Bioscience trends* **3**, 216-219 (2009).

67 Dar, A., Shachar, M., Leor, J. & Cohen, S. Optimization of cardiac cell seeding and distribution in 3D porous alginate scaffolds. *Biotechnology and bioengineering* **80**, 305-312, doi:10.1002/bit.10372 (2002).

68 Roh, J. D. *et al.* Centrifugal seeding increases seeding efficiency and cellular distribution of bone marrow stromal cells in porous biodegradable scaffolds. *Tissue engineering* **13**, 2743-2749, doi:10.1089/ten.2007.0171 (2007).

69 Fernando, H. N. *et al.* Mechanical loading affects the energy metabolism of intervertebral disc cells. *Journal of orthopaedic research : official publication of the Orthopaedic Research Society* **29**, 1634-1641, doi:10.1002/jor.21430 (2011).

70 Yuan, T. Y., Huang, C. Y. & Yong Gu, W. Novel technique for online characterization of cartilaginous tissue properties. *Journal of biomechanical engineering* **133**, 094504, doi:10.1115/1.4004920 (2011).

71 Gu, W. Y., Yao, H., Vega, A. L. & Flagler, D. Diffusivity of ions in agarose gels and intervertebral disc: effect of porosity. *Annals of biomedical engineering* **32**, 1710-1717 (2004).

72 Muller, G. & Hanschke, M. Quantitative and qualitative analyses of proteoglycans in cartilage extracts by precipitation with 1,9-dimethylmethylene blue. *Connective tissue research* **33**, 243-248 (1996).

73 Bashir, A., Gray, M. L., Hartke, J. & Burstein, D. Nondestructive imaging of human cartilage glycosaminoglycan concentration by MRI. *Magnetic resonance in medicine : official journal of the Society of Magnetic Resonance in Medicine / Society of Magnetic Resonance in Medicine* **41**, 857-865 (1999).

74 Lesperance, L. M., Gray, M. L. & Burstein, D. Determination of fixed charge density in cartilage using nuclear magnetic resonance. *Journal of orthopaedic research : official publication of the Orthopaedic Research Society* **10**, 1-13, doi:10.1002/jor.1100100102 (1992).

75 von der Mark K, G. V., von der Mark H, Muller P. Relationship between cell shape and type of collagen synthesised as chondrocytes lose their cartilage phenotype in culture. *Nature* **267**, 531-532 (1977).

76 Gu, W. Y., Lai, W. M. & Mow, V. C. Transport of fluid and ions through a porous-permeable charged-hydrated tissue, and streaming potential data on normal bovine articular cartilage. *Journal of biomechanics* **26**, 709-723 (1993).

77 Grad, S., Eglin, D., Alini, M. & Stoddart, M. J. Physical stimulation of chondrogenic cells in vitro: a review. *Clinical orthopaedics and related research* **469**, 2764-2772, doi:10.1007/s11999-011-1819-9 (2011).

78 Schulz, R. M. & Bader, A. Cartilage tissue engineering and bioreactor systems for the cultivation and stimulation of chondrocytes. *European biophysics journal : EBJ* **36**, 539-568, doi:10.1007/s00249-007-0139-1 (2007).

79 Wang, P. Y., Chow, H. H., Lai, J. Y., Liu, H. L. & Tsai, W. B. Dynamic compression modulates chondrocyte proliferation and matrix biosynthesis in chitosan/gelatin scaffolds. *Journal of biomedical materials research. Part B, Applied biomaterials* **91**, 143-152, doi:10.1002/jbm.b.31384 (2009).

80 Raimondi, M. T. *et al.* The effect of media perfusion on three-dimensional cultures of human chondrocytes: integration of experimental and computational approaches. *Biorheology* **41**, 401-410 (2004).

81 Tran, S. C., Cooley, A. J. & Elder, S. H. Effect of a mechanical stimulation bioreactor on tissue engineered, scaffold-free cartilage. *Biotechnology and bioengineering* **108**, 1421-1429, doi:10.1002/bit.23061 (2011).

82 Khan, A. A., Suits, J. M., Kandel, R. A. & Waldman, S. D. The effect of continuous culture on the growth and structure of tissue-engineered cartilage. *Biotechnol Prog* **25**, 508-515, doi:10.1002/btpr.108 (2009).

83 Waldman, S. D., Usprech, J., Flynn, L. E. & Khan, A. A. Harnessing the purinergic receptor pathway to develop functional engineered cartilage constructs. *Osteoarthritis and cartilage / OARS, Osteoarthritis Research Society* **18**, 864-872, doi:10.1016/j.joca.2010.03.003 (2010).

84 Ng, K. W. *et al.* Transient supplementation of anabolic growth factors rapidly stimulates matrix synthesis in engineered cartilage. *Annals of biomedical engineering* **39**, 2491-2500, doi:10.1007/s10439-011-0356-8 (2011).

85 Knudson, C. B. & Knudson, W. Cartilage proteoglycans. *Seminars in cell & developmental biology* **12**, 69-78, doi:10.1006/scdb.2000.0243 (2001).

86 Bush, P. G. & Hall, A. C. The volume and morphology of chondrocytes within non-degenerate and degenerate human articular cartilage. *Osteoarthritis and cartilage / OARS, Osteoarthritis Research Society* **11**, 242-251 (2003).

87 Becerra, J. *et al.* Articular cartilage: structure and regeneration. *Tissue engineering. Part B, Reviews* **16**, 617-627, doi:10.1089/ten.TEB.2010.0191 (2010).

88 Archer, C. W. & Francis-West, P. The chondrocyte. *The international journal of biochemistry & cell biology* **35**, 401-404 (2003).

89 Knecht, S., Vanwanseele, B. & Stussi, E. A review on the mechanical quality of articular cartilage - implications for the diagnosis of osteoarthritis. *Clin Biomech (Bristol, Avon)* **21**, 999-1012, doi:10.1016/j.clinbiomech.2006.07.001 (2006).